FIELD EMISSION IN A MAGNETIC FIELD

Thesis for the Degree of Ph. D.
MICHIGAN STATE UNIVERSITY
Dennis Jack Flood
1967



This is to certify that the

thesis entitled

FIELD EMISSION IN A MAGNETIC FIELD

presented by

Dennis Jack Flood

has been accepted towards fulfillment of the requirements for

Ph.D degree in Physics

Major professor

Date 34 25 1967



ABSTRACT

FTELD EMISSION IN A MAGNETIC FIELD

by Dennis J. Flood

A theoretical calculation of the field-emission current density in a magnetic field at low temperatures is made using the effective mass approximation to the free-electron The results indicate a monotonically decreasing model. dependence of current density on magnetic field, on which is superimposed a small oscillatory component periodic in The calculation is made only for the case in which the magnetic field is parallel to the electric field. Insertion of suitable values for the quantities appearing in the expression indicates that sizeable oscillations in the current should be obtainable if a substance with a small electronic effective mass is used for the cathode. Experiments performed at liquid helium temperatures (4.2 °K). with magnetic fields ranging up to 20 Kilogauss, failed to show the expected behavior to an accuracy of 5 per cent. Instabilities in the steady dc current level prevented the attainment of better accuracy. An attempt is made to explain the apparent contradiction between experiment and theory by considering the applicability of the theoretical expression to the actual physical situation encountered.

FIELD EMISSION IN A MAGNETIC FIELD

Ву

Dennis Jack Flood

A THESIS

Submitted to
Michigan State University
in partial fulfillment of the requirements
for the degree of

DOCTOR OF PHILOSOPHY

Department of Physics

1967

D1411111 6/6/51

Acknowledgements

I wish to express my sincere appreciation to Professor F.J. Blatt for his help and encouragement throughout this project.

I wish also to thank Dr. M. Garber for his assistance with many experimental problems in the early stages of the research.

Special thanks go to Dr. P.A. Schroeder for providing many helpful insights and much moral support during several of the experimental runs.

I am indebted to Michigan State University and the National Science Foundation for financial support throughout the entire project.

Table of Contents

			Page
1.	Int	troduction	1
2.	Theory		
	Α.	The Field Emission Current in Zero Magnetic Field	3
	B.	Influence of a Magnetic Field	14
3.	Experimental Techniques		
	Α.	Apparatus	29
	В.	Sample Preparation	35
4.	Res	sults	38
5.	Conclusion		49

Figures

		Page
1.	Effective potential energy of an electron	
	near a metallic surface	5
2.	Potential barrier, illustrating classically	
	forbidden region for a particle with energy $\epsilon_{_{ m Z}}$	8
3.	Field emission chamber for use with super-	
	conducting solenoid	30
4.	Field emission chamber for use with iron-core	
	electromagnet	31
5a.	Schematic of high voltage vacuum feed-through	32
5b.	Circuit diagram for electrometer differential	
	amplifier with cathode follower output	32a
5c.	Schematic diagram of the measuring circuit	32a
6.	Field emission current from a zinc cathode	42
7.	Field emission current from a bismuth cathode	42
8.	Current vs. voltage plot for a bismuth cathode	
	in zero magnetic field	44
9.	Current vs. voltage plot for a zinc cathode in	
	zero magnetic field	44
10.	Current vs. voltage plot for a tungsten cathode	
	in zero magnetic field	45
11.	Current vs. voltage plot for a lead-telluride	
	cathode in zero magnetic field	45
12a.	Molecule near a metallic surface in zero	
	applied electric field	57
12b.	Molecule near a metallic surface with an	
	applied electric field	57



1. Introduction

The emission of electrons from a cold cathode into vacuum is a relatively elementary effect which has been understood for some time. The effect was probably observed and noted in many experiments involving high voltages and sharply pointed cathodes, but the first to describe it in detail was R.W. Wood¹⁾ in 1897. Attempts to give an explanation based on classical physics²⁾ were unsuccessful, predicting not only the wrong field dependence, but also a temperature dependence which was not observed³⁾. Millikan and Lauritsen⁴⁾ discovered that the measured current-voltage characteristics could be described by

$$I = Ae^{-B/F}$$
 (1)

where A and B are constants and F is the electric field at the surface of the cathode. Hence a plot of log I versus 1/F gave a straight line, a result which classical theory was totally unable to predict.

The first real advance in an understanding of the phenomenon was made in 1928 by Fowler and Nordheim, 5) who applied quantum theory to the problem. They assumed that the electrons in the metal obeyed Fermi-Dirac statistics and calculated the number of electrons in each range of energy arriving at the surface potential barrier from the inside of the metal. The barrier potential assumed by Fowler and Nordheim was simply a potential step at the metal surface with zero applied field, and a triangular hump in



high field. They solved the Schroedinger equation to find the fraction of electrons which penetrated the barrier. Integrating the product of the number of incident electrons and probability of penetration over all electron energies gave them the following formula for the emitted current density:

$$J = \frac{4 \ln \Phi}{\eta + \Phi} \frac{e^{3} F^{2}}{8 \pi h \Phi} \exp\left(\frac{-8\pi \ln \Phi^{3/2}}{3 h e F}\right) . \tag{2}$$

The quantity -e is the electronic charge, η is the energy of the Fermi level inside the metal relative to the bottom of the conduction band, ϕ is the thermionic work function, and h is Planck's constant. Nordheim later refined the calculation to include the image force on an escaping electron, which resulted in a slightly lower field strength F necessary for the same current density predicted above.

Field emission is, then, simply a barrier penetration phenomenon in which electrons with energies below the Fermi surface tunnel through the narrow potential barrier. The purpose of this paper is to investigate the effect of an externally applied magnetic field on the emission current. Some kind of influence is almost certainly to be expected because of the drastic effect such a magnetic field has on the energies of the conduction electrons inside the metal.

2. Theory

A. The Field Emission Current in Zero Magnetic Field

The F-N (Fowler-Nordheim) Theory assumes that the conduction electrons in a metal form a gas of free particles described by Fermi-Dirac statistics. Accordingly, the possible states of a single particle in a small volume v of the metal may be divided into groups at energies $\mathbf{E}_{\mathbf{i}}$, containing $\mathbf{g}_{\mathbf{i}}$ states populated by $\mathbf{n}_{\mathbf{i}}$ electrons. The distribution formula has the familiar form

$$n_{i} = \frac{g_{i}}{\exp(\frac{E_{i}-\eta}{kT})+1}, \qquad (1)$$

where η is the Fermi energy. The number of states g_i is simply $2v/h^3$ $dp_x dp_y dp_z$, a consequence of the theorem that in each volume h^3 of phase space there are two states for a free particle of spin 1/2. We then have for the number of electrons within volume v and with momenta in the range $dp_x dp_y dp_z$

$$dn = \frac{2v}{h^{2}} \frac{dp_{x}dp_{y}dp_{z}}{exp(\frac{E-\eta}{kT}) + 1} .$$
 (2)

The energy and momentum are related by

$$p_x^2 + p_y^2 + p_z^2 = 2m(E-V)$$
 (5)

where V is the potential energy of an electron of mass m in v.

Following the procedure of the F-N theory, we shall consider a one-dimensional potential which is assumed to have the same effect on a conduction electron as the actual

- metal. There are three contributions to the resulting potential energy of an electron of charge -e:
- (1) In the absence of an applied field, the potential energy inside the metal is equal to zero and has some constant value $\pm W_a$ when the electron and metal are separated.
- (2) With the origin chosen on the surface of the metal and the positive z axis perpendicular to it, an applied electric field F in the z direction gives a contribution -eFz.
- (3) The image force on an electron outside the metal, which arises because of the induced charge on the surface of the metal, gives a contribution $-e^2/4z$. We thus have

$$V(z) = \begin{cases} 0, & z < 0 \\ W_{a} - eFz - e^{2}/4z, & z > 0 \end{cases}$$
 (4)

for the effective potential energy. A plot of this potential energy for a representative case is shown in figure 1.

The next step is to find the equilibrium flux of electrons incident upon the surface of the metal, and then to find the probability that an electron will penetrate the barrier. The emission current of electrons can then be found by integrating the product of the incident flux and penetration probability over all electron energies. From eq. (3) the z part of the total energy of an electron is

$$\epsilon_{z} = E - \frac{p_{x}^{2}}{2m} - \frac{p_{y}^{2}}{2m} = \frac{p_{z}^{2}}{2m} \div V(z) . \tag{5}$$

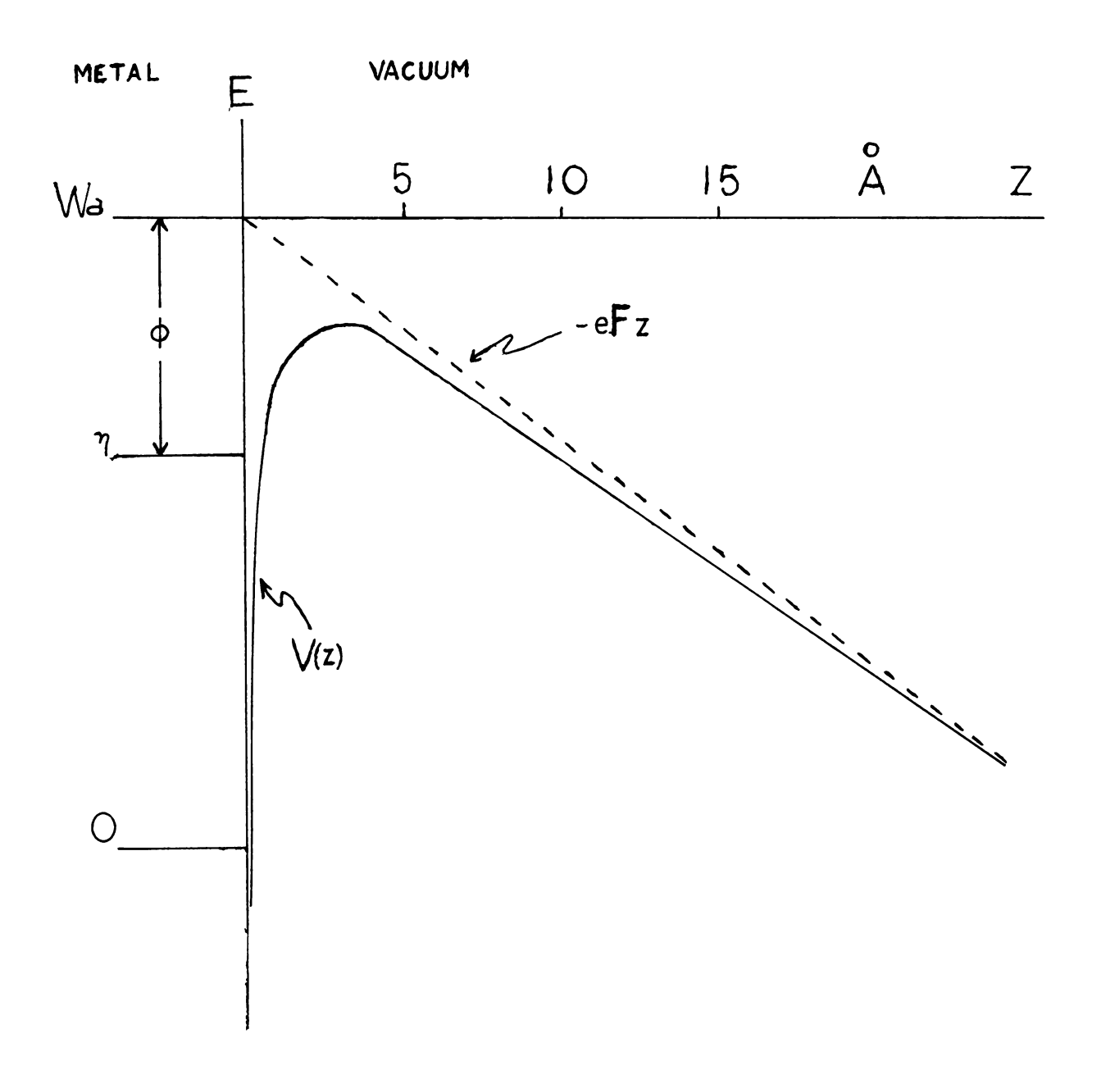


Figure 1 Effective potential energy V(z) of an electron near a metal surface.

The flux of electrons in the z direction with momenta within dp_z is found by multiplying the number of electrons per unit volume with momenta in $dp_x dp_y dp_z$ by $v_z = p_z/m$ and integrating over $\mathrm{dp}_{_{X}}$ and $\mathrm{dp}_{_{y}}.$ Thus, if $\mathrm{N}(\varepsilon_{_{Z}})\mathrm{d}\varepsilon_{_{Z}}$ is the number of electrons with z part of their energy in $\text{d}\varepsilon_{_{\textstyle Z}}$ incident on the surface per second per unit area, we have

$$N(\epsilon_{z})d\epsilon_{z} = \int_{x}^{\infty} \int_{y}^{\infty} \frac{p_{z}}{m} \frac{2}{h^{3}} \frac{dp_{x}dp_{y}dp_{z}}{\exp(\frac{E-\eta}{kT})+1}$$
(6)

or, since inside the metal

$$d\epsilon_{z} = \frac{p_{z}dp_{z}}{m} , \qquad (7)$$

get $N(\epsilon_z)d\epsilon_z = \frac{2}{h^3} d\epsilon_z \int_{-\infty}^{\infty} \frac{dp_x dp_y}{exp(\frac{\epsilon_z - \eta}{1/\eta} + \frac{p_x^2 + p_y^2}{kT}) + 1}.$ we get

(8)

Eq. (8) can be integrated very easily by setting

$$p_{x} = r \cos\theta$$
 (9a)

$$p_{y} = r \sin \theta. \tag{9b}$$

The result is that

$$N(\epsilon_{z}) = \frac{4\pi m kT}{h^{3}} \log \left[1 + \exp\left(\frac{\epsilon_{z} - \eta}{kT}\right)\right]$$
 (10)

Eq. (10) is the appropriate expression to use in the absence of an external magnetic field.

The presence of an external magnetic field will alter the situation considerably. Before considering its effects, however, we shall continue with our discussion of the original Fowler-Nordheim theory, and calculate the probability that an electron with energy in $d\epsilon_z$ impinging upon the barrier will penetrate it. We first note that the Schroedinger equation is

$$\frac{-\hbar^2}{2m} \frac{d^2 \psi(z)}{dz^2} + V(z)\psi(z) = \varepsilon_z \psi(z) \tag{11}$$

or

$$\frac{\mathrm{d}^2 \psi}{\mathrm{d}z^2} - \frac{2\mathrm{m}}{\hbar^2} \left[\epsilon_z - V(z) \right] \quad \psi = 0. \tag{12}$$

Now inasmuch as the emitted electrons come mostly from below the Fermi level at low temperatures, the region of interest here, their energy is far enough from the maximum value of V(z) to enable us to use a WKB approximation to find the transmission coefficient. In this approximation separate solutions to the Schroedinger equation are obtained for the classical regions of motion to the left and right of the barrier, and for the classically forbidden region inside the barrier. Figure 2 shows a potential barrier of arbitrary shape with the appropriate regions indicated for a particle of energy ϵ_z . The time independent wave functions for the three regions are

$$\frac{A}{|k(z)|} \exp(i \int_{a}^{z} kdz) + \frac{B}{|k(z)|} \exp(-i \int_{a}^{z} kdz), \quad z < a$$

$$\psi(z) = \frac{C}{|\gamma(z)|} \exp(-\int_{a}^{z} \gamma dz) + \frac{D}{|\gamma(z)|} \exp(\int_{a}^{z} \gamma dz), \quad a < z < b$$

$$\frac{F}{|k(z)|} \exp(i \int_{b}^{z} kdz) + \frac{G}{|k(z)|} \exp(-i \int_{b}^{z} kdz), \quad z > b$$
(13)

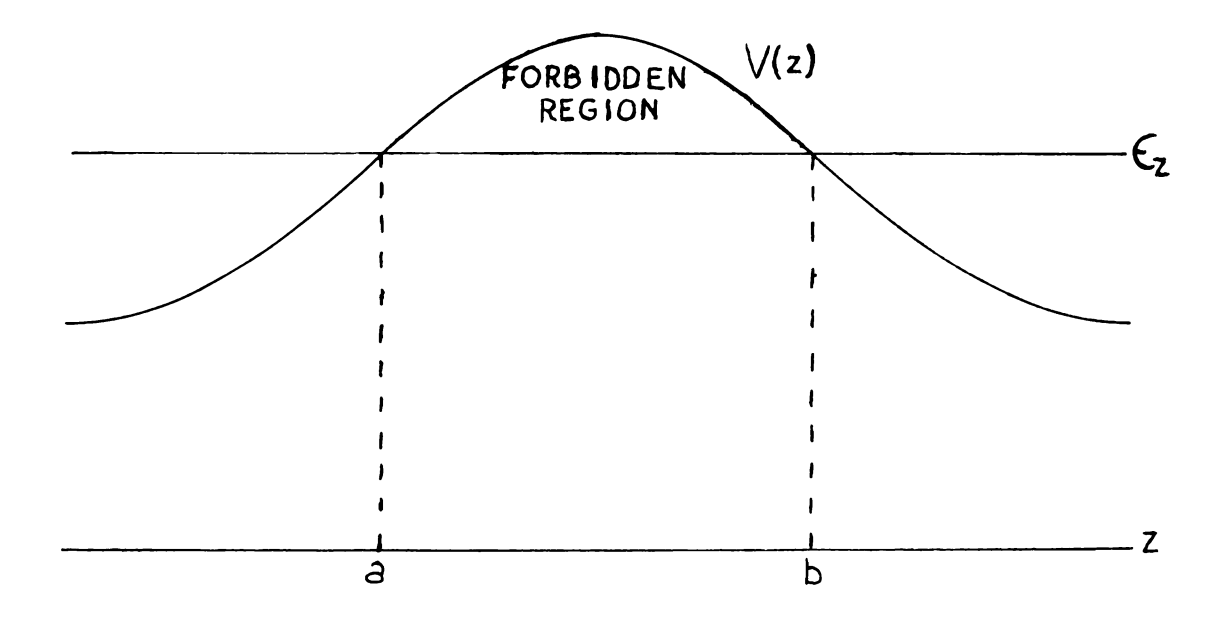


Figure 2 Potential barrier, illustrating classically forbidden region for particle with energy ϵ_z .

$$k(z) = \left[\frac{2m}{n^2} \in_{Z} - v(z)\right]^{1/2} \text{ for } \in_{Z} > V(z),$$
(14a)

$$\gamma(z) = \left[\frac{2m}{\hbar^2} V(z) - \epsilon_{\underline{z}}\right]^{1/2} \text{ for } \epsilon_{\underline{z}} < V(z).$$
 (14b)

The coefficients in (13) are related by the connection formulas at the classical turning points of the motion, i.e., at a and b in figure 2. These are 7)

$$\frac{2}{\mathrm{lk}(z)} \cos\left(\int_{z}^{a} \mathrm{k}(z) dz - \pi/4\right) \longleftrightarrow \frac{1}{\mathrm{l}\gamma(z)} \exp\left(-\int_{a}^{z} \gamma(z) dz\right) \tag{15a}$$

$$\frac{1}{\mathrm{lk}(z)} \sin\left(\int_{z}^{a} \mathrm{k}(z) dz - \pi/4\right) \longleftrightarrow \frac{-1}{\mathrm{l}\gamma(z)} \exp\left(\int_{a}^{z} \gamma(z) dz\right) \tag{15b}$$

when the turning point is to the right of the classical motion, and

$$\frac{1}{|\gamma(z)|} \exp(-\int_{z}^{b} \gamma(z) dz) \longleftrightarrow \frac{2}{|k(z)|} \cos(\int_{b}^{z} k(z) dz - \pi 4)$$

$$(16a)$$

$$\frac{-1}{|\gamma(z)|} \exp(\int_{z}^{b} \gamma(z) dz \longleftrightarrow \frac{1}{|k(z)|} \sin(\int_{b}^{z} k(z) dz - \pi / 4)$$

$$(16b)$$

when the turning point is to the left of the classical motion. The double arrow indicates the proper direction of application of the formulas when admixtures of the solutions in the various regions are unknown.

The transmission coefficient is defined by

$$D = \frac{|\psi \text{trans}|^2 \quad \text{vtrans}}{|\psi \text{inc}|^2 \quad \text{vinc}}.$$
 (17)

We assume no wave moving to the left for z > b so (17) becomes simply

$$D = \frac{|F|^2}{|A|^2} \tag{18}$$

where, by use of the connection formulas,

$$A = \frac{1}{2} \left(2\Theta + \frac{1}{2\Theta} \right) F \tag{19}$$

with

$$\Theta = \exp\left(\int_{a}^{b} \gamma(z) dz.$$
 (20)

Hence

$$D = \frac{4}{(2\theta + \frac{1}{2\theta})^2}$$
 (21)

and for $\theta >> 1$, which corresponds to a high and broad barrier,

$$D \doteq \frac{1}{\theta^2} = \exp(-2\int_a^b \gamma(z) dz = \exp(-\int_a^b \left[\frac{8m}{h^2}\right] (V(z) - \epsilon_z)^{1/2} dz$$
(22)

As a check on the validity of our approximations we note from (4) that the maximum value of V(z) occurs at

$$z_{o} = \frac{1}{2} \sqrt{\frac{e}{F}}$$
 (23)

and has the value

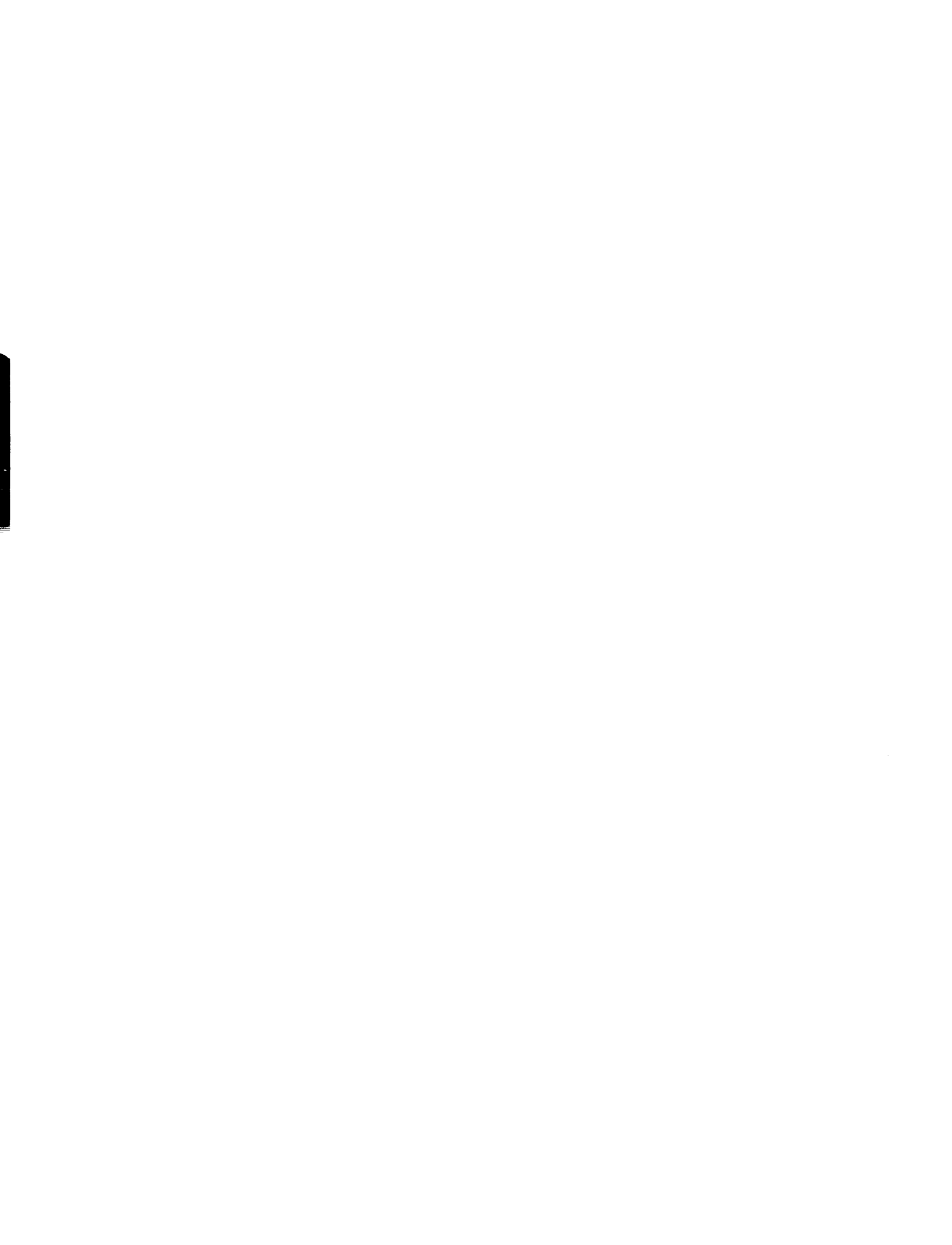
$$V_{\text{max}} = W_{\text{a}} - e^{3}F$$
 (24)

For an applied field of 5×10^7 volts/cm, or 1.67×10^5 statvolts/cm, (24) gives

$$W_{a} - V_{max} = 2.68ev$$
, (25)

while a typical value for $W_a - \eta$ is $\phi \doteq 4 \, \text{ev}$. Hence the height of the barrier will always be above the Fermi level for the electric fields normally used.

We must now evaluate the expression for the transmission coefficient for electrons impinging on the barrier. This



was first done by Nordheim⁶⁾ in 1928 and later improved upon by Burgess, Kroemer, and Houston.⁸⁾ Taking the logarithm of eq. (22), we get

$$-LnD = \int_{z_1}^{z_2} \sqrt{\frac{8m}{\hbar^2} (W_a - eFz - e^2/4z - \epsilon_z)} dz$$
(26)

where z_1 and z_2 are the classical turning points of the barrier. (In this region $W_a - \epsilon_z > 0$.) Solving eq. (4) for $V(z) = \epsilon_z$ in the region z > 0 will give us z_1 and z_2 . The result is

If the change of variable

$$\sigma = \frac{2eF}{W_a - \epsilon_z} z \tag{28}$$

and the parameter

$$y = \frac{\sqrt{e^3 F}}{W_a - \epsilon_z} \tag{29}$$

are introduced, eq. (26) becomes

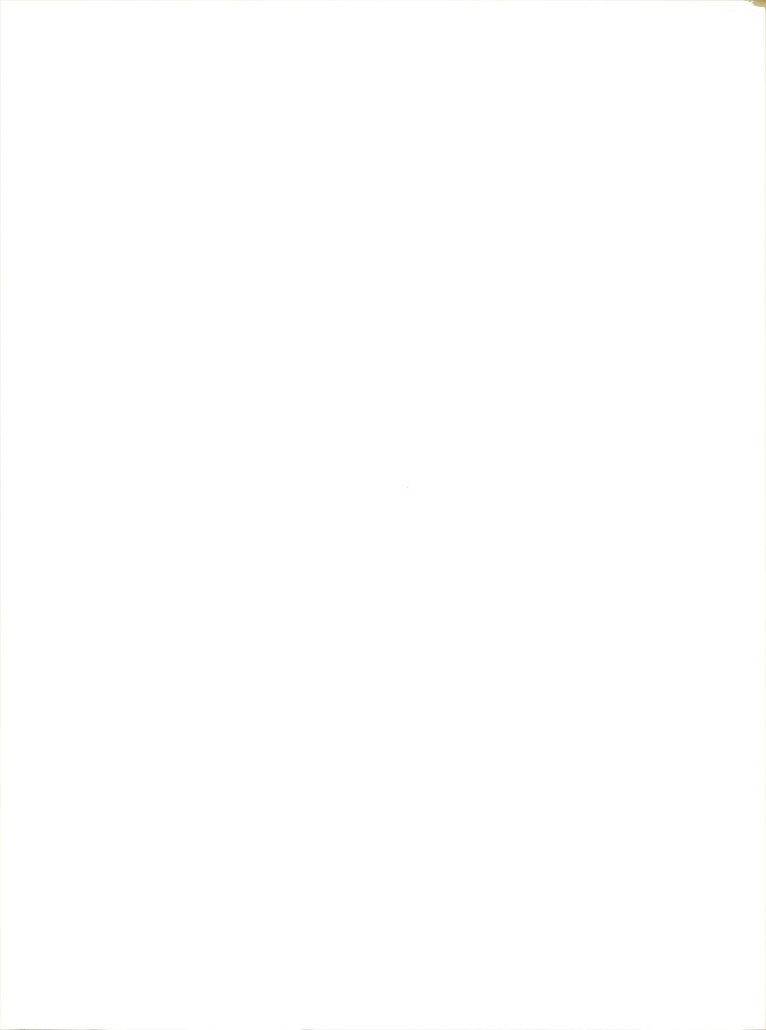
$$-\operatorname{LnD} = \int_{1-\sqrt{1-y^2}}^{1+\sqrt{1-y^2}} \sqrt{\frac{8m}{n^2} \left(-\sigma \frac{W_a - \epsilon_z}{2} + W_a - \epsilon_z - \frac{e^3 F}{2\sigma (W_a - \epsilon_z)}\right)} \frac{W_a - \epsilon_z}{2eF} d\sigma$$

$$= \frac{\sqrt{m(W_a - \epsilon_z)^3}}{heF} \int_{1-\sqrt{1-y^2}}^{1+\sqrt{1-y^2}} \sqrt{-\sigma^2 + 2\sigma - y^2} \frac{d\sigma}{\sigma}.$$
(30)

Substituting

$$q = \sqrt{\sigma} \tag{31}$$

into (30) gives



$$-LnD = \frac{2\sqrt{m(W_a - \epsilon_z)^3}}{\hbar eF} \int_{b}^{a} \sqrt{-q^4 + 2q^2 - y^2} dq$$

$$= \frac{2\sqrt{m(W_a - \epsilon_z)^3}}{\hbar eF} \int_{b}^{a} \sqrt{(a^2 - q^2)(q^2 - b^2)} dq$$
(32)

where

$$a = \sqrt{1 + \sqrt{1 - y^2}}$$
 (33a)

$$b = \sqrt{1 - \sqrt{1 - y^2}}$$
 (33b)

so that

$$-a^2b^2 = y^2 \tag{34a}$$

$$a^2 + b^2 = 2$$
 (34b)

Eq. (32) is in a standard form for an elliptic integral and has been evaluated. ⁹⁾ The result is

$$-LnD = \frac{4\sqrt{m(W_a - \epsilon_z)^3}}{3heF} a \left[\frac{a^2 + b^2}{2} E(k) - b^2 K(k) \right]$$
 (35)

where

$$k^{2} = \frac{a^{2} - b^{2}}{a^{2}} = \frac{2\sqrt{1 - y^{2}}}{1 + \sqrt{1 - y^{2}}}$$
(36)

and K and E are the complete elliptic integrals of the first and second kinds:

$$K(k) = \int_{0}^{\pi/2} \frac{d\phi}{\sqrt{1-k^2 \sin^2 \phi}}$$
 (37a)

$$E(k) = \int_{0}^{\pi/2} \sqrt{1 - k^2 \sin^2 \phi} d\phi$$
 (37b)

In terms of the parameter y, eq. (35) gives

$$D = \exp\left(\frac{-4\sqrt{2m(W_{a} - \epsilon_{z})^{3}}}{3heF} \frac{\sqrt{1 - \sqrt{1 - y^{2}}}}{\sqrt{2}} \left[E(k) - (1 - 1 - y^{2})K(k) \right] \right)$$

$$= \exp\left(\frac{-4\sqrt{2m(W_{a} - \epsilon_{z})^{3}}}{3heF} v(y) \right)$$
 (38)

where

$$v(y) = \sqrt{\frac{1}{2}} \sqrt{1 + \sqrt{1 - y^2}} \left[E(k) - (1 - \sqrt{1 - y^2}) K(k) \right].$$
 (39)

As mentioned earlier, most of the emitted electrons will have energies near the Fermi level, so we may expand the exponent in (38) around $\epsilon_{\rm Z}$ = n, and retain only the first two terms as a sufficient approximation. Hence, with

$$W_{a} - \eta = \phi$$

$$4/3 \sqrt{\frac{2m(W_{a} - \epsilon_{z})^{3}}{neF}} v(y) = 4/3 \sqrt{\frac{2m\phi^{3}}{neF}} v(\frac{e^{3}F}{\phi}) + \frac{2\sqrt{2m\phi}}{neF} \left[v(\frac{\sqrt{e^{3}F}}{\phi}) + \frac{2\sqrt{2m\phi}}{neF} \left[v(\frac{$$

But

$$dy = \frac{\sqrt{e^3 F}}{(W_0 - v_z)^2} d\varepsilon_z = \frac{y}{W_0 - \varepsilon_z} d\varepsilon_z$$
(41)

and

$$\frac{d\mathbf{v}(\mathbf{y})}{d\epsilon_{\mathbf{z}}} = \div \frac{\mathbf{y}}{W_{\mathbf{a}} - \epsilon_{\mathbf{z}}} \frac{d\mathbf{v}(\mathbf{y})}{d\mathbf{y}} \tag{42}$$

so (40) becomes

$$-\frac{4}{3} \frac{\sqrt{2m(W_a - \epsilon_z)^{\frac{3}{5}}}}{\text{heF}} v(y) \doteq -\frac{4}{3} \sqrt{2m} \frac{\frac{\sqrt{3}}{2}}{\text{heF}} v(y) - \frac{2\sqrt{2m\phi}}{\text{heF}} t(y) (\epsilon_z - n)$$
(43)

where

$$t(y) = v(y) - (2/3)y \frac{dv(y)}{dy}$$
 (44)

We finally obtain

$$D = \exp(-g + \frac{\epsilon_z - \eta}{d}) \tag{45}$$

with

$$g = 4/3 \sqrt{2m} \frac{\phi^{3/2}}{heF} v(y) = 6.83 \times 10^7 \frac{\phi^{3/2}}{F} v(y)$$
 (46a)

$$d = \frac{heF}{2\sqrt{2m\phi t(y)}} = 9.76 \times 10^{-9} F/\phi^{1/2}t(y)$$
 (46b)

when ϕ is in electron-volts and F in volts/cm.

B. Influence of a Magnetic Field

In the absence of a magnetic field the z part of the electron's total energy is given by eq. (5), and to find the emission current for such a case we must simply insert the expression for ϵ_z into the right sides of equations (10) and (45), take their product, multiply by the electronic charge -e and velocity \mathbf{v}_z , and integrate over all values of ϵ_z . It is at this point that we depart from the F-N Theory, for we must now investigate what happens to the electronic energy in the presence of an externally applied magnetic field. We shall use the effective mass approximation to the free electron theory.

The one-electron Hamiltonian for an electron in a magnetic field is

$$\mathcal{H} = \frac{1}{2m^*} \left(\bar{p} + \frac{e}{c} \bar{A} \right)^2 + V(z) \tag{47}$$

where m* is the effective mass, \bar{p} the electron momentum, -e the electronic charge, and \bar{A} the vector potential. For a magnetic field in the z direction we set

$$\bar{A} = \mathcal{J}_{Hx}$$
 (48)

and obtain in (47)

$$\mathcal{H} - V(z) = \frac{1}{2m^*} \left[p^2 + \frac{e}{c} (\bar{p} \cdot \bar{A} + \bar{A} \cdot \bar{p}) + \frac{e^2}{c^2} A^2 \right]
= \frac{1}{2m^*} \left[p_x^2 + p_y^2 + 2 \frac{e}{c} p_y H_x + \frac{e^2 H^2 x^2}{c^2} + p_z^2 \right]
= \frac{1}{2m^*} \left[p_x^2 + (p_y + \frac{eH}{c} x)^2 + p_z^2 \right].$$
(49)

Replacing classical variables by the appropriate quantum mechanical operators we obtain, for the time independent Schroedinger equation

$$\left[\frac{-\dot{\mathbf{n}}^2(\frac{\partial^2}{\partial \mathbf{x}^2} + \frac{\partial^2}{\partial \mathbf{z}^2}) + \frac{1}{2m^*}(-\dot{\mathbf{n}}\frac{\partial}{\partial \mathbf{y}} + \frac{e\mathbf{H}}{c}\mathbf{x})^2 + \mathbf{V}(\mathbf{z})\right] \psi = \epsilon \psi$$
(50)

If we set, noting that V(z) = 0 in this case,

$$\Psi = \exp(ik_y y) \exp(ik_z z) X(x)$$
 (51a)

$$k_z^2 = \frac{2m^*}{5^2} \epsilon_z \tag{51b}$$

we obtain

$$\left[\frac{\hbar^{2}}{2m^{*}}(k_{y}^{2}+k_{z}^{2})+\frac{1}{2m^{*}}(-\hbar^{2}\frac{\partial 2}{\partial x^{2}}-2\hbar k_{y}^{2}m^{*}\omega x+m^{*}^{2}\omega^{2}x^{2})\right]X=\epsilon X$$
(52)

with

$$\omega = -eH/m*c (53)$$

From (52)
$$\left[\frac{-\hbar^2}{2m^*} \frac{\partial^2}{\partial x^2} - \hbar k_y \omega x + \frac{m^* \omega^2 x^2}{2}\right] X = \left[\epsilon - \frac{\hbar^2}{2m^*} (k_y^2 + k_z^2)\right] X = EX$$
(51)

Setting

$$x = x + \frac{\hbar k_y}{m * \omega} \tag{55}$$

gives

$$\left[\frac{-\hbar^{2}}{2m^{*}}\frac{d^{2}}{dx^{2}} - \hbar k_{y}\omega x' - \frac{\hbar^{2}k_{y}^{2}}{m^{*}} + \frac{m^{*}\omega^{2}x^{2}}{2} + \hbar k_{y}\omega x' + \frac{\hbar^{2}k_{y}^{2}}{2m^{*}}\right]X = EX$$
(56)

This is the standard equation of a simple harmonic oscillator centered at

$$x_0 = -\frac{\hbar k_y}{m * \omega} \tag{58}$$

with eigenvalues

$$E' = (n+1/2)\hbar\omega, \quad n = 0,1,2,3,....$$
 (59)

But

$$E' = E + \frac{\hbar^2 k_y^2}{2m^*} = \epsilon - \frac{\hbar^2 k_z^2}{2m^*}$$
 (60)

SO

$$\epsilon = \hbar \omega (n+1/2) + \frac{\hbar^2 k_z^2}{2m^*}$$
 (61)

From (61) we obtain, with $\epsilon_z = \hbar^2 k_z^2/2m^*$,

$$\epsilon_z = \epsilon - \hbar\omega(n + 1/2) = \epsilon - \epsilon_n$$
 (62)

for the z part of the electron's energy inside the metal.

We must now find the number of states with quantum number n and energy between ϵ_z and $\epsilon_z+d\epsilon_z$. The degeneracy of a state with quantum numbers n and k_z is determined by the allowed values of k_y . The range of these values can be found by requiring that x_o , the center-point of the motion of the oscillator, fall within the boundaries of

the specimen. Assuming a rectangular box of sides $\mathbf{L}_{x},$ $\mathbf{L}_{y},$ and $\mathbf{L}_{z},$ with the origin of coordinates at the center, we obtain

$$(-1/2)L_{x} < x_{o} < (1/2)L_{x}$$
 (63)

or

$$\frac{m^*\omega L_x}{2\hbar} < k_y < -\frac{m^*\omega L_x}{2\hbar}$$
 (64)

which may be rewritten as

$$-\frac{\text{eHL}_{x}}{2\text{hc}} < k_{y} < \frac{\text{eHL}_{x}}{2\text{hc}}. \tag{65}$$

The number of k_y values in the above range is, then, (assuming periodic boundary conditions)

$$\delta n_{y} = \delta k_{y} \left(\frac{L_{y}}{2\pi}\right) = \frac{eH}{2\pi hc} L_{x}L_{y} . \tag{66}$$

The number of allowed $k_{_{\rm Z}}$ values in a plane slab of thicknes $\delta k_{_{\rm Z}}$ perpendicular to $k_{_{\rm Z}}$ is just $(L_{_{\rm Z}}/2\pi)\delta k_{_{\rm Z}}$. Hence the total number of allowed $k_{_{\rm Z}}$ and $k_{_{\rm Z}}$ values for a given n, i.e. the degeneracy of the state n, is just

$$\delta n_{n} = \delta n_{y} \delta n_{z} = \frac{L_{x} L_{y} L_{z}}{4\pi^{2}} \frac{eH}{\hbar c} \delta k_{z} . \qquad (67)$$

But we may write

$$k_{z} = \frac{(2m^{*})^{1/2}}{\tilde{n}} \epsilon_{z}^{1/2} \tag{68}$$

SO

$$dk_z = \frac{(2m^*)^{1/2}}{2\hbar} \epsilon_z^{-1/2} d\epsilon_z \tag{69}$$

Hence the number of states per unit volume in the energy range ϵ_z to ϵ_z + d ϵ_z , with a given n, is

$$N_{n}(\epsilon_{z})d\epsilon_{z} = 2 \frac{eH}{h^{2}} (2m^{*})^{1/2} \epsilon_{z}^{-1/2} d\epsilon_{z}, \qquad (70)$$

and the flux of electrons incident upon the barrier is simply

$$S_{n}(\epsilon_{z})d\epsilon_{z} = \frac{1}{2} f(\epsilon_{z}, \epsilon_{n}) v_{z} N_{n}(\epsilon_{z}) d\epsilon_{z} , \qquad (71)$$

where $f(\varepsilon_z, \varepsilon_n)$ is the Fermi distribution function. The factor 1/2 is inserted because for a given n and ε_z only half of the electrons will have $v_z > 0$.

The expression for the total emission current density in this case now assumes the form

$$\begin{split} \mathbf{J} &= \frac{1}{2} \int_{0}^{\infty} \sum_{n=0}^{\infty} \mathbf{f}(\boldsymbol{\varepsilon}_{z}, \boldsymbol{\varepsilon}_{n}) \mathbf{N}_{n}(\boldsymbol{\varepsilon}_{z}) \mathbf{v}_{z} \mathbf{D}(\boldsymbol{\varepsilon}_{z}) d\boldsymbol{\varepsilon}_{z} \\ &= \frac{2e^{2}H}{h^{2}c} \int_{0}^{\infty} \mathbf{D}(\boldsymbol{\varepsilon}_{z}) \left[\sum_{n=0}^{\infty} \left(\exp(\frac{\boldsymbol{\varepsilon}_{z} + \boldsymbol{\varepsilon}_{n} - \boldsymbol{\eta}}{kT}) + 1 \right)^{-1} \right] d\boldsymbol{\varepsilon}_{z} \end{aligned}$$

Substituting for $D(\epsilon_z)$ from eq. (45),

$$J = \frac{2e^{2}H}{h^{2}c} \exp(-g-\eta/d) \int_{0}^{\infty} \exp(\varepsilon_{Z}/d) \left[\sum_{n=0}^{\infty} \left(\exp\left(\frac{\varepsilon_{Z} + \hbar\omega(n+1/2) - \eta}{kT} \right) + 1 \right)^{-1} \right] d\varepsilon_{Z}.$$
(75)

We shall made use of Poisson's summation formula to evaluate the sum over n in eq. (73). To this end we set

$$\exp\left(\frac{\epsilon_{Z} - \eta}{kT}\right) = B \tag{74}$$

and obtain

$$\begin{split} \sum_{n=0}^{\infty} \left(\text{B} \, \exp\!\left(\frac{\hbar \omega (n+1/2)}{kT} \right) \, + \, 1 \right)^{-1} &= \, \lim_{y \to \infty} \int_{0}^{y} \frac{\text{d}x}{\text{B} \, \exp\!\left(\frac{\hbar \omega x}{kT} \right) + 1} \\ &+ \, 2 \sum_{S=1}^{\infty} (-1)^{S} \int_{0}^{\infty} \frac{\cos 2\pi Sx}{\text{B} \, \exp\!\left(\hbar \omega x / kT \right) \, + \, 1} \end{split} \tag{75}$$

The first integral in eq. (76) is simply

$$I_{1} = \int_{0}^{y} \frac{dx}{E \exp(\frac{\hbar \omega x}{kT}) + 1} = y - \frac{kT}{\hbar \omega} Ln(1+E) \exp(\frac{\hbar \omega y}{kT}) + \frac{kT}{\hbar \omega} Ln(1+E)$$
(76)

For y >> $kT/\hbar\omega$, however,

$$\operatorname{Ln}\left[1+\operatorname{B}\exp(\frac{\hbar\omega y}{kT}\right] \doteq \operatorname{LnB}\exp(\frac{\hbar\omega y}{kT}) = \frac{\hbar\omega y}{kT} + \operatorname{LnB} \tag{77}$$

SO

$$\lim_{y\to\infty} \mathbf{I}_1 = \frac{kT}{\hbar\omega} \operatorname{Ln} \frac{1+B}{B} = \frac{kT}{\hbar\omega} \operatorname{Ln}(\exp(\frac{\eta^{-\varepsilon}\mathbf{z}}{kT}) + 1). \tag{78}$$

The second integral has the form

$$I_2 = \int_0^{\infty} f(x) \cos 2\pi Sx \, dx \tag{79}$$

and becomes, after an integration by parts,

$$I_{2} = \frac{f(x)}{2\pi S} \sin 2\pi Sx \Big|_{0}^{\infty} - \frac{1}{2\pi S} \int_{0}^{\infty} \frac{\partial f}{\partial x} \sin 2\pi Sx \quad dx \quad . \tag{80}$$

The first term vanishes at both limits and we are left with the second term only. Although the integral in eq. (81) appears to be of the form

$$I = \int_{0}^{\infty} \frac{\partial f(E)}{\partial E} g(E) dE , \qquad (81)$$

it may not be evaluated by the procedures commonly employed for such integrals because the integrand oscillates very rapidly in the region of the fermi surface. We may, however, make use of the fact that $-\partial f/\partial x$ has a sharp maximum of width kT about the value X' such that

$$\epsilon(\mathbf{X}, \epsilon_{\mathbf{Z}}) = \hbar\omega\mathbf{X} + \epsilon_{\mathbf{Z}} = \eta$$
 (82)

where $\boldsymbol{\eta}$ is the Fermi energy. If we redefine the origin so that

$$x = X' + \xi \tag{83}$$

we get

$$f(x, \epsilon_z) = \exp(\frac{\hbar\omega\xi}{kT} + 1)^{-1} . \tag{84}$$

Now if we set

$$equation = \frac{\hbar\omega}{kT}\xi \tag{85}$$

eq. (81) becomes

$$I_{2} = \frac{-1}{2\pi S} \int_{0}^{\infty} \sin 2\pi S(X + \rho \frac{kT}{\hbar \omega}) \frac{\partial f}{\partial \rho} d\rho . \tag{86}$$

We may, without introducing a serious error, extend the lower limit in (86) to $-\infty$. Then

$$I_{2} = \frac{-\sin 2\pi SX}{2\pi S} \int_{-\infty}^{\infty} \cos \frac{2\pi SkT\rho}{\hbar\omega} \frac{\partial f}{\partial \rho} d\rho$$

$$-\frac{\cos 2\pi SX}{2\pi S} \int_{-\infty}^{\infty} \sin \frac{2\pi SkT\rho}{\hbar\omega} \frac{\partial f}{\partial \rho} d\rho \qquad (87)$$

But $-\partial f/\partial \rho$ is an even function of ρ , so we are left with

$$I_{2} = \frac{+\sin 2\pi SX}{2\pi S} \int_{-\infty}^{\infty} \cos(\frac{2\pi SkT\varrho}{\hbar\omega}) (\frac{1}{\exp(\varrho/2) + \exp(-\varrho/2)})^{2} d\varrho$$

$$= \frac{+\sin 2\pi SX}{2\pi S} \int_{-\infty}^{\infty} \frac{\cos(\frac{2\pi SkT\varrho}{\hbar\omega})}{4\cosh^{2}\varrho/2} d\varrho$$

$$= \frac{+1}{2\pi S} \sin 2\pi SX \frac{\frac{2\pi^{2}SkT}{\hbar\omega}}{\sin \frac{2\pi^{2}SkT}{\hbar\omega}}.$$
 (88)

Inserting eqs. (78) and (88) into (73) gives

$$J = \frac{2e^{2}H}{h^{2}c} \exp(-g-\eta/d) \int_{0}^{\infty} \exp(\frac{\epsilon_{z}}{d}) \left[\frac{kT}{\hbar\omega} \ln(\exp(\frac{\eta-\epsilon_{z}}{kT}) + 1\right]$$

$$+\sum_{S=1}^{\infty} (-1)^{S} \frac{\sin(2\pi S \frac{\eta - \epsilon_{Z}}{\hbar \omega})}{\pi S} \frac{2\pi^{2} SkT}{\hbar \omega} d\epsilon_{Z}$$

$$= \sinh(\frac{2\pi^{2} SkT}{\hbar \omega}) d\epsilon_{Z}$$
(89)

where we have used the fact that

$$X = \frac{\eta - \epsilon_{Z}}{\tilde{n}\omega} \qquad (90)$$

The range of integration in eq. (69) should in actual fact be cut off at $\epsilon_z = V(z)_{max}$, since for $\epsilon_z > V(z)_{max}$, $D(\epsilon_z) = 1$ and we are in the thermionic region. Actually, not much error will be introduced if the upper limit is set equal to η , the fermi energy. To this approximation, then, we have

$$\frac{Jh^2c\hbar\omega}{2kTe^2H\exp(-g-\frac{\eta}{d})} = \int_0^{\eta} \exp(\frac{\epsilon_z}{d}) \ln(\exp(\frac{\eta-\epsilon_z}{kT}) + 1) d\epsilon_z$$

$$+ 2\pi \sum_{S=1}^{\infty} (-1)^{S} \frac{1}{\sinh(\frac{2\pi^{2}SkT}{\hbar\omega})} \int_{0}^{\eta} \exp(\frac{\epsilon_{Z}}{d}) \sin(2\pi S \frac{\eta - \epsilon_{Z}}{\hbar\omega}) d\epsilon_{Z}.$$
(91)

Consider the second integral first. This may be rewritten as

$$I_{2}^{I} = \int_{0}^{\eta} \exp(\frac{\epsilon_{z}}{d}) \left(\sin \frac{2\pi S_{r}}{\hbar \omega} \cos \frac{2\pi S \epsilon}{\hbar \omega} z - \cos \frac{2\pi S_{r}}{\hbar \omega} \sin \frac{2\pi S \epsilon}{\hbar \omega} z\right) d\epsilon_{z}.$$
(92)

Set

$$2\pi S \frac{\eta}{\hbar \omega} = \Theta \qquad . \tag{93}$$

Then

$$I_{2}^{I} = \frac{\exp(\frac{\epsilon_{Z}}{d}) \left[\frac{1}{d} \cos \frac{2\pi S \epsilon_{Z}}{\hbar \omega} + \frac{2\pi S}{\hbar \omega} \sin \frac{2\pi S \epsilon_{Z}}{\hbar \omega} \right] \sin \theta}{\left(\frac{1}{d} \right)^{2} + \left(\frac{2\pi S}{\hbar \omega} \right)^{2}}$$

$$= \frac{\exp(\frac{\epsilon_{Z}}{d}) \left[\frac{1}{d} \sin \frac{2\pi S \epsilon_{Z}}{\hbar \omega} - \frac{2\pi S}{\hbar \omega} \cos \frac{2\pi S \epsilon_{Z}}{\hbar \omega} \right] \cos \theta}{\left(1/d \right)^{2} + \left(2\pi S/\hbar \omega \right)^{2}}$$

$$= \left[\frac{2\pi S}{\hbar \omega} \exp(\frac{r}{d}) - \frac{1}{d} \sin \frac{2\pi S r}{\hbar \omega} - \frac{2\pi S}{\hbar \omega} \cos \frac{2\pi S r}{\hbar \omega} \right] \frac{1}{\left(\frac{1}{d} \right)^{2} + \left(\frac{2\pi S}{\hbar \omega} \right)^{2}}$$

$$(94)$$

Evaluation of the first integral will be facilitated if we set

$$B' = \exp(\frac{n}{kT}) \tag{95}$$

and make the change of variable

$$y = \exp(\frac{\epsilon}{d}z)$$
; $dy = \frac{1}{d}yd\epsilon_z$. (96)

Now since

$$\operatorname{Ln}\left[1+\operatorname{B}'\exp(\frac{\epsilon_{Z}}{\operatorname{kT}})\right] = \operatorname{Ln}\exp(\frac{-\epsilon_{Z}}{\operatorname{kT}})\left(\exp(\frac{\epsilon_{Z}}{\operatorname{kT}})+\operatorname{B}'\right)$$

$$= \frac{-\epsilon_{Z}}{\operatorname{kT}} + \operatorname{Ln}(\exp(\frac{\epsilon_{Z}}{\operatorname{kT}})+\operatorname{B}'), \quad (97)$$

the first integral in (91) becomes

$$I_{1}^{I} = \int_{1}^{e^{\eta/d}} dLn(y^{d/kT} + B') dy - \int_{0}^{\eta} exp(\frac{\epsilon_{z}}{d})(\frac{-\epsilon_{z}}{kT}) d\epsilon_{z} . (98)$$

The second integral in (93) is simply

$$I_1^{II} = -\frac{1}{kT} (d)^2 \exp(\frac{\pi}{d})(\frac{\pi}{d} - 1) - \frac{(d)^2}{kT}$$
 (99)

while the first becomes

$$I_{1}^{III} = d \int_{1}^{e^{\eta/d}} \frac{\frac{d}{kT}}{E'} + 1) dy + d(exp(\frac{\eta}{d}) - 1) LnB'$$
(100)

Performing an integration by parts on the remaining integral gives

$$I_{1}^{\text{IV}} = d \exp\left(\frac{\eta}{d}\right) \ln 2 - d \ln\left(\exp\left(\frac{-\eta}{kT}\right) + 1\right)$$

$$- \frac{d \exp\left(\frac{-\eta}{kT}\right)}{kT} \int_{0}^{\eta} \frac{\exp\left(\frac{\varepsilon_{Z}}{kT}\right)}{\exp\left(\frac{\varepsilon_{Z}-\eta}{kT}\right) + 1} d\varepsilon_{Z}, \qquad (101)$$

and finally,

$$I_{1}^{V} = \frac{-d \exp(\frac{-r}{kT})}{kT} \int_{0}^{\eta} \frac{\exp(\frac{\varepsilon}{kT})}{\exp(\frac{(\varepsilon_{Z} - \eta)}{kT}) + 1} d\varepsilon_{Z}$$

$$= -d \ln 2 + d \ln \left(\exp(\frac{\eta}{kT}) + 1\right) , \qquad (102)$$

so that

$$I_1^I = .693d(\exp(\frac{\eta}{d}) - 1) - \frac{d}{kT} \left[d(\exp(\frac{\eta}{d}) - 1) - \eta \right].$$
 (103)

Eq. (92) becomes, at last

$$J = \frac{2e^{2}H}{h^{2}c} \exp(-g - \frac{\eta}{d})d\left\{\frac{1}{h\omega}\left[.693kT(\exp(\frac{\eta}{d}) - 1)\right] + \frac{1}{d}\sum_{s=1}^{\infty}(-1)^{s}\frac{2\pi^{2}s\frac{kT}{h\omega}}{\sin\left(\frac{2\pi^{2}skT}{h\omega}\right)}\right\}$$

$$\frac{2}{(\frac{1}{d})^{2}+(\frac{2\pi s}{h\omega})^{2}}\left[\exp(\frac{\eta}{d}) - \cos\frac{2\pi s\eta}{h\omega} - \frac{\hbar\omega}{2d\pi s}\sin\frac{2\pi s\eta}{h\omega}\right]$$

$$(104)$$

Oscillations in the field emission current density, periodic in 1/H, are readily apparent from eq. (104).

The entire derivation above makes use of the assumption that the Fermi level is independent of the magnetic field. Such will be the case only if the number of electrons in the conduction band is allowed to vary. This situation is

often encountered in practice, however, when a light effective-mass conduction band overlaps a high density-of-states, heavy effective-mass hole band. Bismuth and many other semi-metals exhibit this kind of overlapping band structure, in which the hole band will accommodate electrons from or contribute them to, the conduction band. If, however, the number of electrons is fixed, then the Fermi level will vary as the magnetic field is changed. This will be the case if there is no band overlap at all, a circumstance not often found except in monovalent metals and suitably doped semiconductors.

If η_0 represents the Fermi energy at $T=0^{\circ}_K$ in zero magnetic field, then for constant electron concentration the Fermi energy is given by 10)

$$\eta = \eta_{0} \left[1 - \frac{1}{12} \left(\frac{\pi k T}{r_{0}} \right)^{2} - \frac{1}{80} \left(\frac{\pi k T}{\eta_{0}} \right)^{4} + \frac{1}{48} \left(\frac{\hbar c}{\eta_{c}} \right)^{2} + \frac{1}{384} \left(\frac{\pi k T \hbar \omega}{\eta_{0}} \right)^{2} - \frac{\pi k T (\hbar \omega)^{1/2}}{\sqrt{2} \left(\frac{\pi k}{\eta_{0}} \right)^{3/2}} \sum_{q=1}^{\infty} \frac{(-1)^{q}}{\sqrt{q}} \frac{\sin(\frac{2\pi q \eta}{\hbar \omega} - \frac{\pi}{4})}{\sinh(\frac{2\pi^{2} q k T}{\hbar \omega})} \right].$$
(105)

It is this expression which must be used in eq. (104) for evaluating the emission current when the electron concentration is fixed.

For metals, semi-metals, and degenerate semiconductors of small effective mass, the temperature dependence at low temperatures is not terribly great, so for that reason it becomes convenient and instructive to examine the expression for the current density in the limit $T \longrightarrow O^C K$. From eq. (104)

$$\begin{split} J &= \frac{2e^2H}{h^2c} \exp(g - \frac{\eta}{d})d \left\{ \frac{d(\exp(\frac{\eta}{d}) - 1) - \eta}{h\omega} \right. \\ &+ \sum_{S=1}^{\infty} (-1)^S \frac{2h\omega/d}{(\frac{h\omega}{d})^2 + 4\eta^2S^2} \left[\exp(\frac{\eta}{d}) - \cos\frac{2\pi S\eta}{h\omega} \right. \\ &- \frac{h\omega}{d} \frac{1}{\pi S} \sin\frac{2\pi S\eta}{h\omega} \right\}. \end{split} \tag{106}$$

If we choose a typical value of $F = 3 \times 10^7 \text{ V/cm}$ for the electric field, and consider substances in which $m^* = 10^{-2} \text{m}_{\odot}$

$$g = 1.43$$
 (107a)

$$\hbar\omega = g^*H \doteq 1.1 \times 10^{-3}H \text{ ev}$$
 (107c)

and we see that for reasonable values of the magnetic field,

$$\hbar\omega/d \ll 1$$
 . (108)

Hence to the lowest order in has/d, eq. (106) becomes

$$\begin{split} \mathbf{J} &\doteq \frac{2\mathrm{e}^2 \mathbf{H}}{\mathrm{h}^2 \mathrm{c}} \, \exp(-\mathrm{g} - \frac{\eta}{\mathrm{d}}) \, \mathrm{d} \left[\frac{\mathrm{d} (\exp(\frac{\eta}{\mathrm{d}}) - 1) - \eta}{\mathrm{h} \omega} \right. \\ &- \sum_{S=1}^{\infty} (-1)^S \, \frac{2(\frac{\mathrm{h}\omega}{\mathrm{d}})}{2\pi^2 \mathrm{S}^2} \, (\exp(\frac{\eta}{\mathrm{d}}) - \cos\frac{2\pi \mathrm{S} \eta}{\mathrm{h} \omega}) \right] \, . \end{split} \tag{109}$$

Furthermore it often happens that $\eta << d$ for such materials, so we may use η/d as an expansion parameter also, obtaining

$$\begin{split} \mathbf{J} & \doteq \frac{2e^2H}{h^2c} \, \exp(-g - \frac{\eta}{d}) \, \mathrm{d} \left[\frac{\mathrm{d} \left(\frac{\eta}{d} + \frac{1}{2} \left(\frac{\eta}{d} \right)^2 - \, \eta}{\hbar \omega} \right. \right. \\ & + \left. \sum_{S=1}^{90} \left(-1 \right)^S \, \frac{\hbar \omega}{d} \, \frac{1}{2\pi^2 S^2} \, \left(1 - \, \cos \frac{2\pi S \, \eta}{\hbar \omega} \right) \right. \end{split}$$

$$\frac{1}{2} \frac{4\pi \text{em} + h\omega}{h^{2}} \exp(-g) d \left[\frac{1}{2} \frac{2}{2 d h\omega} + \frac{\hbar \omega}{d} \sum_{S=1}^{\infty} \frac{(-1)^{S}}{2\pi^{2} S^{2}} (1 - \cos \frac{2\pi S \eta}{h\omega}) \right] \\
= \frac{2\pi \text{em} + \eta^{2}}{h^{2}} \exp(-g) \left[1 + 2(\frac{\hbar \omega}{\eta})^{2} \sum_{S=1}^{\infty} \frac{(-1)^{S}}{2\pi^{2} S^{2}} (1 - \cos \frac{2\pi S \eta}{h\omega}) \right]. \tag{110}$$

The above expression was first derived by Blatt, ¹¹⁾ who considered only the case $T=0^{\circ}K$, so that the Fermi distribution function could be set equal to unity for $\epsilon<\eta$, and zero otherwise.

Eq. (110) may be used as it appears above when evaluating the emission current if the Fermi energy does not change with magnetic field. From eq. (105) however, we see that for $T=0^{\circ}k$,

$$\eta = \eta_0 \left[1 + \frac{1}{48} \left(\frac{\hbar \omega}{\eta_0} \right)^2 - \frac{1}{(8\pi^2)^{1/2}} \left(\frac{\hbar \omega}{\eta_0} \right)^{3/2} \sum_{q=3/2}^{(-1)} \sin \left(\frac{2\pi q \eta}{\hbar \omega} - \frac{\pi}{4} \right) \right],$$
(111)

and this expression must be inserted in eq. (110) whenever the assumption of constant Fermi energy is not valid.

Using the same expansion parameters as above, we obtain

$$J = \frac{2\pi e m^* \eta_0^2}{h^2} \exp(-g) \left\{ 1 + \frac{1}{24} \left(\frac{\hbar \omega}{\eta_0} \right)^2 + 2 \left(\frac{\hbar \omega}{\eta_0} \right)^2 \frac{\omega}{S=1} \frac{(-1)^S}{2\pi^2 S^2} \left(1 - \cos \frac{2\pi S \eta_0}{\hbar \omega} \right) \right\}$$

$$+ \frac{1}{(2\pi^2)^{1/2}} \left(\frac{\hbar \omega}{\eta_0} \right)^{3/2} \frac{\omega}{q=1} \frac{(-1)^q}{q^{3/2}} \sin(\frac{2\pi q \eta_0}{\hbar \omega} - \frac{\pi}{4}) \right\}, (112)$$

which differs from eq. (110) essentially only by the presence of an additional field-dependent term. The additional

oscillatory term will dominate the behavior of the current in low magnetic fields ($\hbar\omega << \eta_{o}$), but as $\hbar\omega$ approaches η_{o} , the first oscillatory term will begin to contribute significantly. Since the two terms have a different dependence of amplitude on magnetic field, and differ in phase by a factor of $\pi/4$, experimental identification of the two should be possible.

From the above results we see that a study of the behavior of field emission in a magnetic field ought to give us some information on the nature of the fermi surface of an electronic system. In particular, one should be able to obtain information similar to that given by de Haasvan Alphen techniques on the extremal areas of the Fermi surface. In addition to this the presence of overlapping bands ought to be detectable through the absence or presence of the last term in eq. (112). Furthermore, we may simplify that equation somewhat by noting that

$$\sum_{S=1}^{\infty} \frac{(-1)^{S}}{\pi^{2} S^{2}} = -\frac{1}{12}$$
(113)

and

$$G(x) = x^{2} - \frac{1}{12} = \sum_{S=1}^{\infty} \frac{(-1)^{S}}{\pi^{2}S^{2}} \cos 2\pi xS, -\frac{1}{2} < x < \frac{1}{2},$$
(114)

so that

$$\sum_{S=1}^{2} \frac{(-1)^{S}}{\pi^{2} s^{2}} (1 - \cos \frac{2\pi S \eta}{\hbar \omega}) = -\frac{1}{12} - G(\frac{\eta_{0}}{\hbar \omega}), -\frac{1}{2} < \frac{\eta_{0}}{\hbar \omega} < \frac{1}{2}.$$
(115)

Eq. (112) becomes

$$J = \frac{2\pi e^{\frac{\pi}{\hbar}} e^{\frac{2}{e} - g}}{\hbar^{\frac{3}{2}}} \left\{ 1 - \frac{1}{24} \left(\frac{\hbar \omega}{\eta_0} \right)^2 G\left(\frac{\eta_0}{\hbar \omega} \right) + \left(\frac{1}{2\pi^2} \right)^{\frac{1}{2}} \left(\frac{\hbar \omega}{\eta_0} \right)^{\frac{3}{2}} F\left(\frac{\eta_0}{\hbar \omega} \right) \right\},$$

$$(116)$$

where

$$F\left(\frac{\eta_{0}}{\hbar\omega}\right) = \frac{\infty}{q=1} \frac{\left(-1\right)^{q}}{q^{3/2}} \sin\left(\frac{2\pi\eta_{0}}{\hbar\omega} - \frac{\pi}{4}\right) \tag{117}$$

From this expression we see that a monotonic decrease in the emission current, which is quadratic in H, is also predicted.

We have seen that the application of an external magnetic field does indeed influence the behavior of a field emission current from a cold cathode into vacuum, within the single-particle, free-electron approximation. Furthermore, numerical evaluation of the theoretical expression, using accepted values for the quantities appearing there, indicates that the effects mentioned above ought to be physically observable in appropriate materials. The next section will describe the attempts to verify experimentally the predictions made in the preceeding pages.

3. Experimental

A. Apparatus

Since the interest in this experiment was in the behavior of the total field emission current with magnetic field, and since the experiment had to be performed at liquid helium temperatures in order to observe any quantum effects, no attempt was made to construct the usual type of field emission microscope (FEM). Such a device contains a phosphor screen maintained at anode potential so that the spatial distribution of the current over the cathode may be displayed at tremendous magnification. Furthermore the anode to cathode distance in an FEM is typically on the order of a centimeter or more. Hence, in order to get the required field strengths at the cathode surface it becomes necessary to use very sharp ($\sim 10^{-5}$ cm radius) needle-shaped emiter tips or else very high applied voltages. To avoid the problems imposed by the above requirements, the cathode in this experiment was placed much closer to the anode, typical separations being 1mm or less.

Two different experimental chambers were constructed, one for use with a superconducting solenoid, and the other for use with a conventional laboratory iron-core electromagnet. In both, however, the anode was suspended from a stainless steel tube which extended from a high voltage feed-through in the dewar flange at the top of the apparatus,

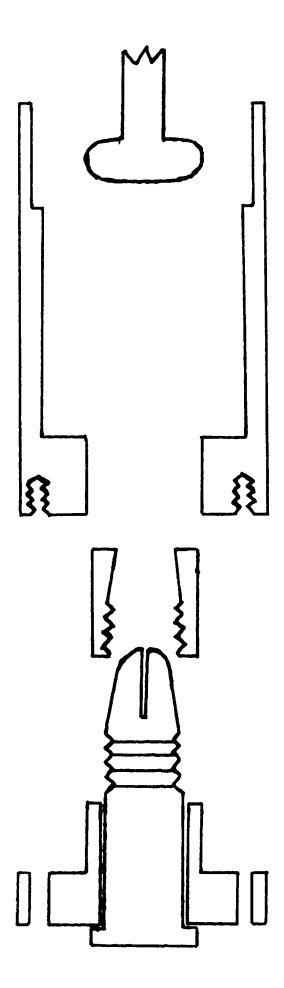
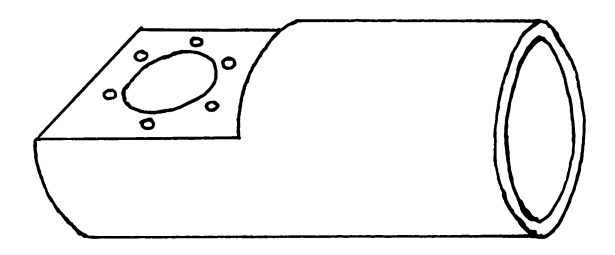


Figure 3 Field emission chamber for use with superconducting solenoi.



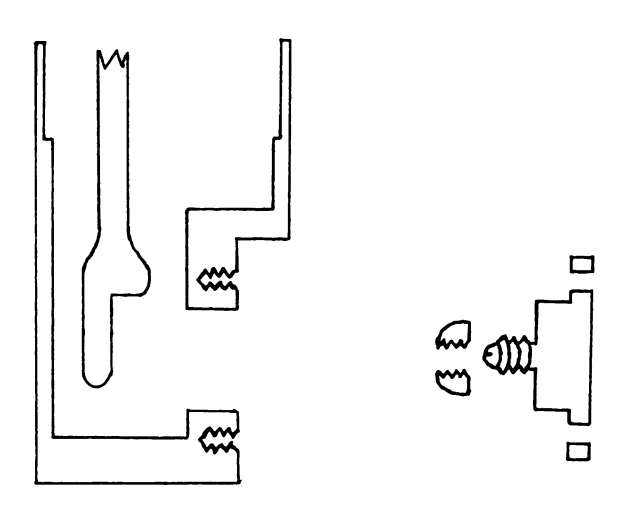


Figure 4 Field emission chamber for use with iron-core electromagnet

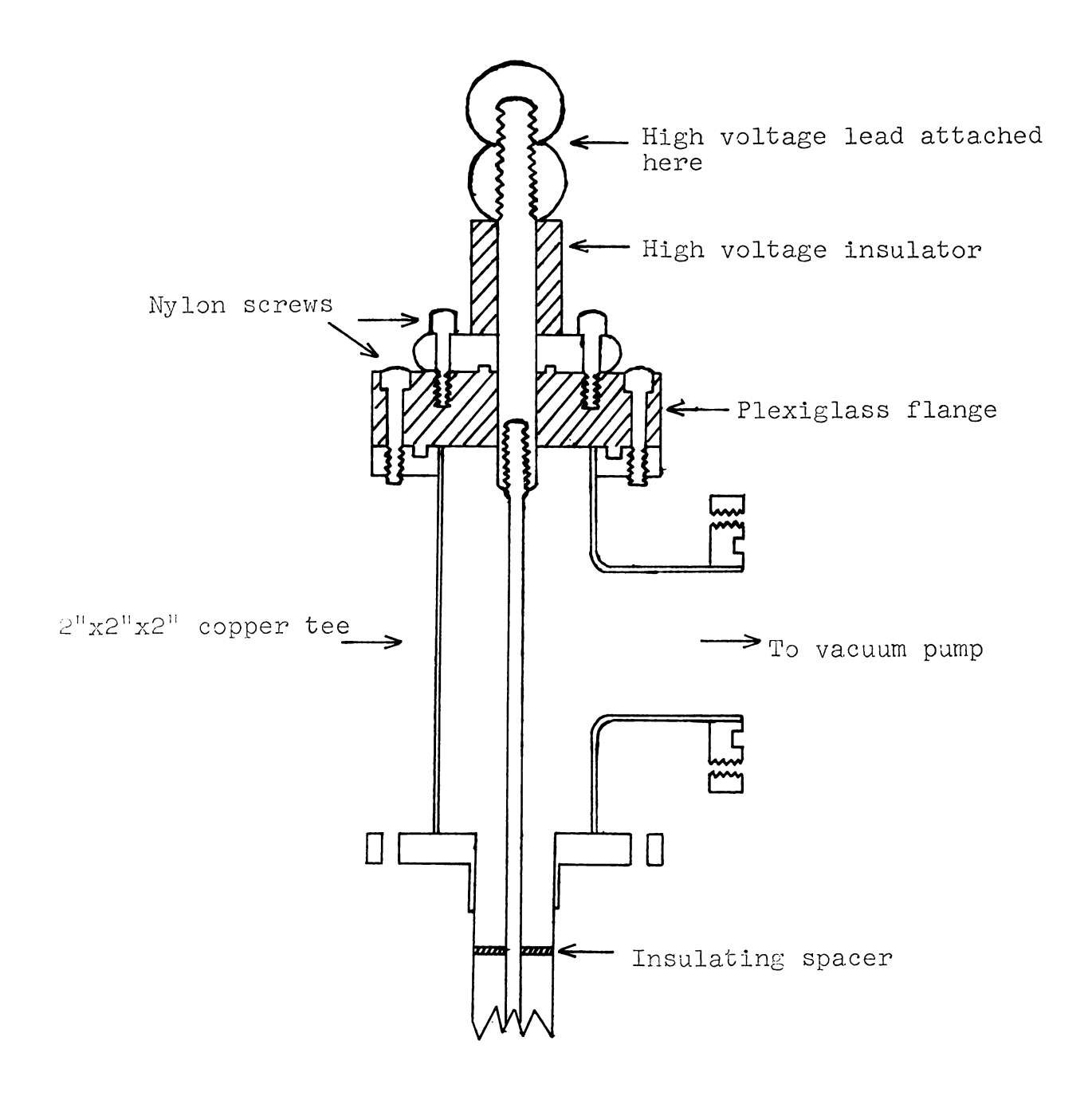
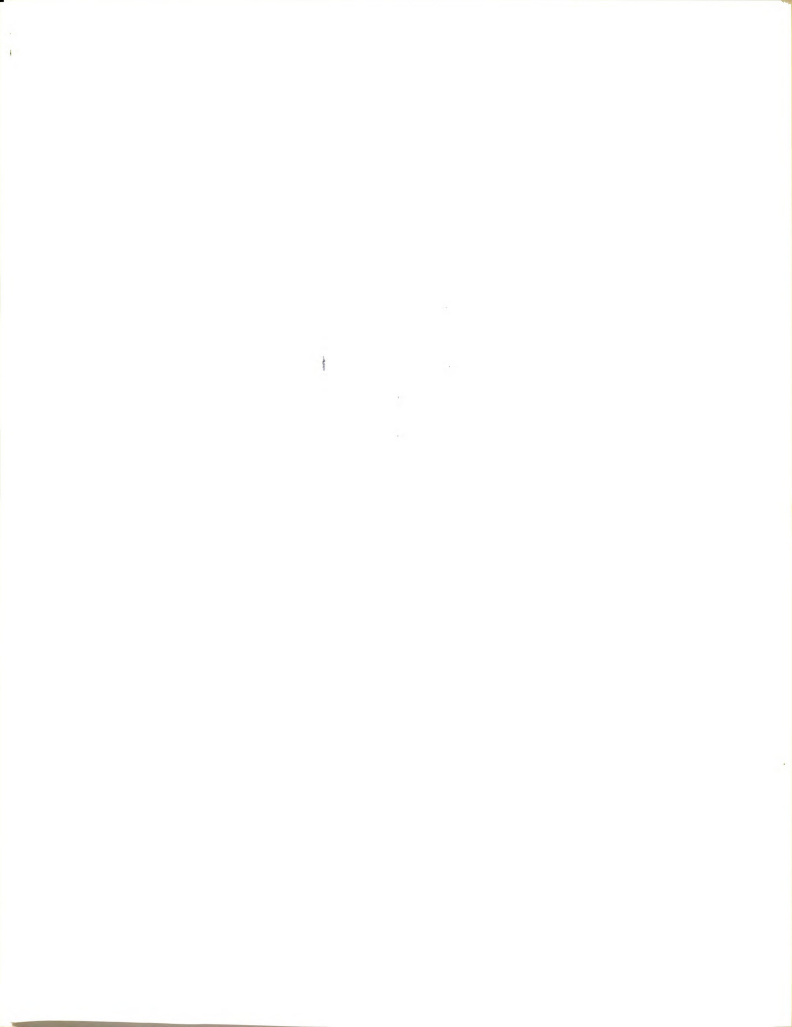


Figure 5a Schematic of high voltage vacuum feed-through.



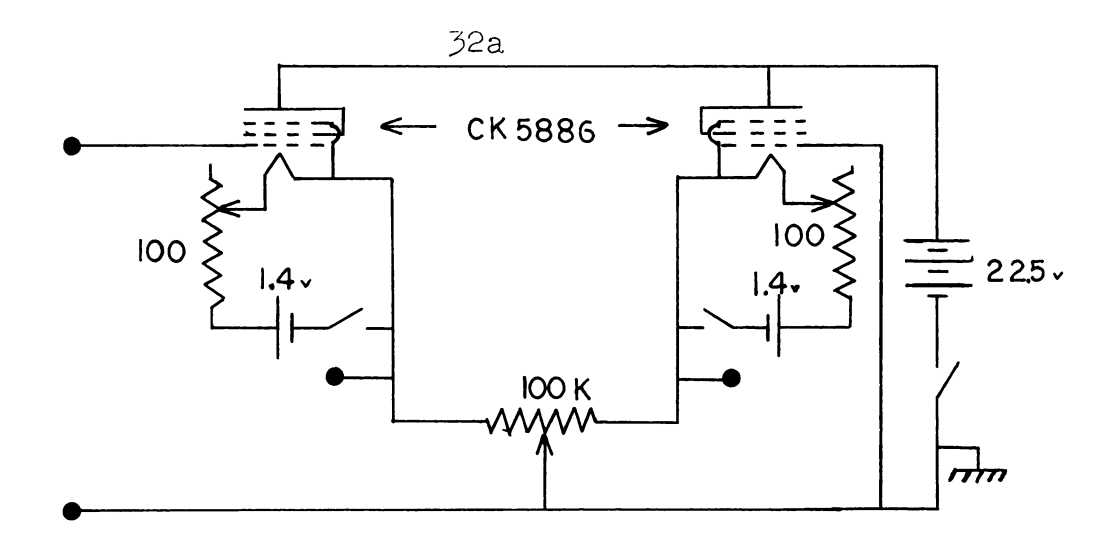


Figure 5b Circuit diagram for electrometer differential amplifier with cathode follower output

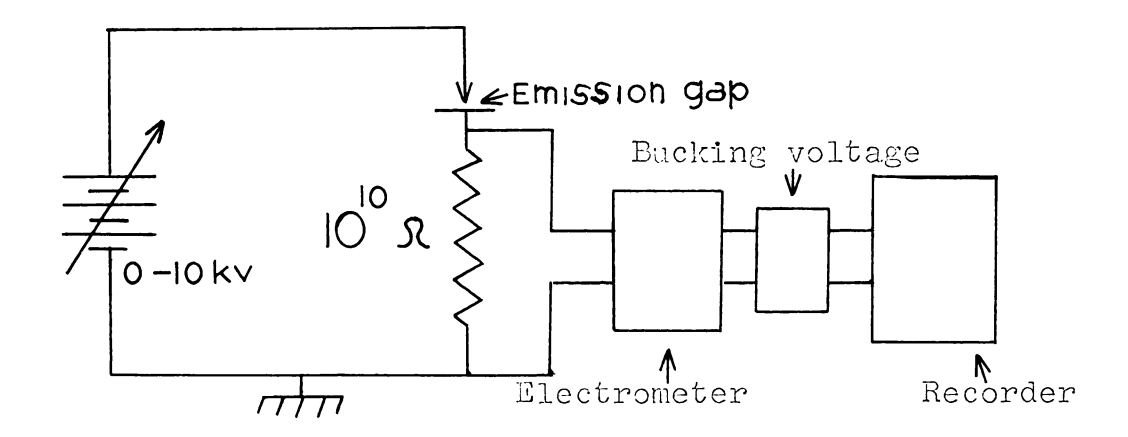


Figure 5c Schematic diagram of the measuring circuit

through the pumping line and into the brass chamber at the bottom. This arrangement was chosen to avoid using a heavily insulated high voltage lead which would have to pass through the bath, an undesirable procedure from several aspects. The stainless steel tube was held rigidly inside the pumping line by several insulating spacers placed along its length. For use with the solenoid the field emission tip had to be mounted with its axis in a vertical position, whereas with the electromagnet the emitter axis had to be horizontal. This was accomplished by constructing the two brass chambers shown in figures 3 and 4. Both arrangements were quite suitable, although eventually use of the solenoid was terminated because of the large amount of liquid helium required to make a single run and also because it was felt that fields up to 20 kgauss would be sufficient. The entire emission chamber was electrically insulated from the pumping line by means of a copper-glass-copper housekeeper seal. The current lead out of the dewar could then be fastened to a bolt on the outside of the chamber, thereby avoiding the use of a glass-to-metal feed-through in the bath.

The sample was mounted in a chuck made from oxygenfree, high-conductivity (OFHC) copper to insure good
thermal contact with the helium bath. In one case the
chuck was soldered into a brass flange which could be
bolted onto the experimental chamber, and in the other case,
the chuck and flange were machined as one piece. A very

reliable vacuum seal was obtained with both arrangements simply by winding a piece of lead wire once around the inside shoulder of the flange, overlapping the ends, and bolting the flange securely into place. This eliminated the necessity of prefabricating a lead o-ring of exact specifications, and of machining a groove in the flange for it.

A differential electrometer amplifier with a cathode follower output was constructed using two Raytheon CK 5886 electrometer tubes, and was used to measure the current. A selection of input resistors from 10^5 to 10^{12} ohms was available through use of a specially constructed, tefloninsulated rotary switch obtained from Kiethely Instruments, Inc. The output of the amplifier went into one channel of a dual pen strip-chart recorder. The combination of recorder amplifier and electrometer allowed, in principle at least, the possibility of measuring currents as low as 10^{-14} amperes. Unfortunately the RC time constant of the circuit became prohibitively large when the input resistance was greater than 10^{10} ohms, so measurements were limited to currents of 10^{-11} amperes or larger.

The magnetic field of the solenoid was swept in a linear fashion by a motor-driven potentiometer in a feedback loop built into the magnet power supply itself. The field of the electromagnet was swept essentially by sending an error signal from an integrator circuit into the feedback loop of that magnet's power supply. A complete description of the latter method for sweeping the magnetic field can be found in reference

12. In either case a signal directly proportional to the field was fed into the other channel of the strip-chart recorder so that a simultaneous display of magnetic field and emission current verses time was possible.

B. Sample Preparation

Principle interest in the experiment centered on the use of bismuth for the field emission cathode, since it was felt that the predicted behavior of the current would be most easily observed in this material. Other materials tried were indium, tungsten, zinc, and lead telluride.

Two methods of preparing bismuth samples were tried. The first, which produced very sharp tips of quite regular geometry, involved the following procedure. A piece of commercial 10 mil bismuth wire (resistance ratio $\frac{R300}{R^4\cdot .2} \doteq 70$) was secured in a temporary chuck with about 1 cm of the wire protruding. The chuck was then fastened in a ringstand clamp with the wire hanging vertically downward. Next a strip of manganin ribbon, which was heated by passing an alternating current of approximately 2 or 3 amps through it, was raised on a small jack-stand until it just touched the bismuth wire. A molten zone then formed at that end of the bismuth wire and grew along its length until it neared the chuck, which acted as a heat sink. At that point the manganin ribbon was slowly and steadily lowered, pulling the end of the bismuth wire with which it was in

contact. This caused the wire to pull apart, leaving a very sharp conical tip on both pieces. The upper piece in the temporary chuck cooled almost immediately and could then be examined under a microscope before being transferred to the sample-holder. The whole operation took about five minutes, and with a little care produced a suitably shaped emitter tip at least once in every three attempts. Furthermore, it was found upon selecting a random one of them and x-raying it, that the polycrystalline wire had formed into a single crystal where the molten zone had passed. Indeed, microscopic examination of every tip made this way showed no gross irregularities in the surface, which strongly supported the belief that they were all single crystals, at least in the region of the actual emitting area.

The other method of preparing a bismuth tip involved starting with a single crystal of known orientation, and then etching it electrochemically in a solution of 2 parts phosphoric acid, 2 parts sulphuric acid, and 1 part distilled water. This process took considerably longer, and did not produce emitter tips which were as sharp or had as regular a geometry as those produced by the first method. Nonetheless, because there was no uncertainty about the nature of the crystal structure of the sample, the second method was used exclusively in the later experimental trials.

Indium was tried as an emitter principally because a tip could be prepared in the same manner as bismuth, i.e.

by heating and pulling it. Tungsten was tried as a matter of course because it is the metal most commonly used as a field emission cathode, and can be shaped into a tip very easily by electrochemically etching it in a sodium-hydroxide solution. Zinc was selected because in certain crystallographic directions it exhibits small effective masses and a large de Haas-van Alphen effect, and again can be prepared quite easily in an electrochemical etch using NaOH. zinc crystal used was oriented along the (0001) direction, which is the direction in which dHvA oscillations are largest. Finally, n-type PbTe was used because it closely approximates the assumptions made in obtaining the expression for the field-emission current. (Effective masses are small, there is no carrier "freeze-out" at low temperatures, and there are no overlapping bands.) Furthermore, cathode tips could be prepared with reasonable ease by electrochemical etching in a solution of potassium dichromate and nitric acid. (4 parts $K_{p}CrO_{7}$ with 1 part HNO_{3}).

4. Results

Before discussing the results obtained from the experiments with each of the above-mentioned materials, a word or two concerning some of the difficulties encountered in making the measurements is in order. The most troublesome problem was that of obtaining a stable field-emission current for an extended period of time. The magnitude of a field emission current at constant voltage depends greatly on the surface condition of the emitter tip, and is extremely sensitive to the presence of adsorbed gases, or to the presence of gases in the emission chamber. Changes in emission current by an order of magnitude or more are not uncommon under poor vacuum conditions, and even under what are considered in many cases good vacuum conditions, (pressures < 10⁻⁶ mm Hg), large (10 - 50 per cent) and sudden changes in the current will occur. The only way to eliminate noise of this nature from the current is to use extremely clean emitter tips, and ultra low pressures ($< 10^{-11}$ mm Hg). In this experiment the emission chamber was first evacuated with a conventional oil diffusion pump to a pressure of approximately 10^{-5} mm Hg. At that point the apparatus was pre-cooled to liquid nitrogen temperature, after which liquid helium was transferred into the dewar. During the pre-cooling period and transfer the valve to the pump was closed and helium gas was admitted into the emission chamber to provide thermal



contact between the anode and outside wall so that both would be cooled simultaneously. Once the transfer was complete the helium gas was pumped out of the system, while everything else was presumed to have condensed on the walls of the chamber.

Even though it was felt that the above procedure should have provided the necessary vacuum for stable field emission, the problem of obtaining clean cathode surfaces still remained. Since bismuth has such a low melting point it was not possible to remove the adsorbates by flashing the tip to a high temperature in vacuum, as is customarily done with, for example, tungsten cathodes. The only other alternative was to remove the contaminating ions from the surface by field desorption techniques. If the cathode is made positive with respect to the anode and at the same time subjected to an intense electric field, positive ions which have been adsorbed on the surface will be stripped away and attracted to the anode. Unfortunately, to achieve significant desorption, field strengths approximately 10 times stronger than those necessary for field emission are required. This often was not possible to achieve with the power supply available for the experiment, which had an output of + 10,000 volts. As a result of this, and the uncertainty of the quality of the vacuum in the chamber, noise levels could not be kept as low as was desired. levels which were within 1 per cent peak-to-peak of the steady dc current levels were sought, but typically the

noise was on the order of 5 per cent peak-to-peak, and this was obtained only after considerable time and patience had been expended in "training" the emitter tip. The "training" consisted of drawing currents of varying amounts for extended periods of time, reversing the polarity of the applied voltage in an effort to induce field desorption, and then checking the current levels again. Such a process usually took several hours during a run and oftentimes the entire run was spent trying to obtain a stable current, with not even a chance to subject it to a magnetic field.

For short periods of time (approx. 1 minute) a relatively stable current could be alloained, so as a result the following procedure for taking data evolved. First an attempt to "train" the emitter was made. If the noise could not be reduced to desirable levels after three or four hours, then a plot of current versus applied voltage in zero magnetic field was made. The high voltage power supply was then put in its standby mode, and the electromagnet turned on and set at some value of magnetic field. Again a plot of current versus voltage, at the same voltages used before, was obtained - a process which took only a few minutes. The high voltage was once more turned off, the magnetic field changed, and the process repeated. (It must be mentioned that at this point any kind of dependence on magnetic field was being sought, since it was felt that noise levels were too high to allow oscillations to be observed.)

Even though the oscillations were deemed difficult to detect, it was still felt that the monotonic decrease in current density which is quadratic in H as given by eq. (116) above, should have been readily observable. fact, however, not a single run on any of the abovementioned metals showed any dependence of field emission current on magnetic field whatsoever, to within an accuracy of at least 5 per cent. Figure 6 shows the behavior of the current drawn from a tip made from the high purity zinc crystal already mentioned. To within the accuracy indicated, no dependence on H can be seen. Similar results were obtained from cathodes made from single crystal bismuth as well. Unfortunately it was very difficult to prevent breakdown when using bismuth, and in every case the data was obtained after a breakdown had occurred. (No breakdown occurred with the zinc crystal, however.) Since a breakdown usually alters the shape of the cathode considerably, interpretation of these results is somewhat in question. It is possible that the breakdown in each case may have altered the crystal structure in the region near the emitting surface to such a degree that considerable scattering of the electrons may have washed out any dependence on magnetic field. However, since the actual region from which electrons are emitted is so small, the current could still have originated from a single crystal area, even though the bulk of the tip region consisted of several crystals of different orientation. At any rate it is a question which



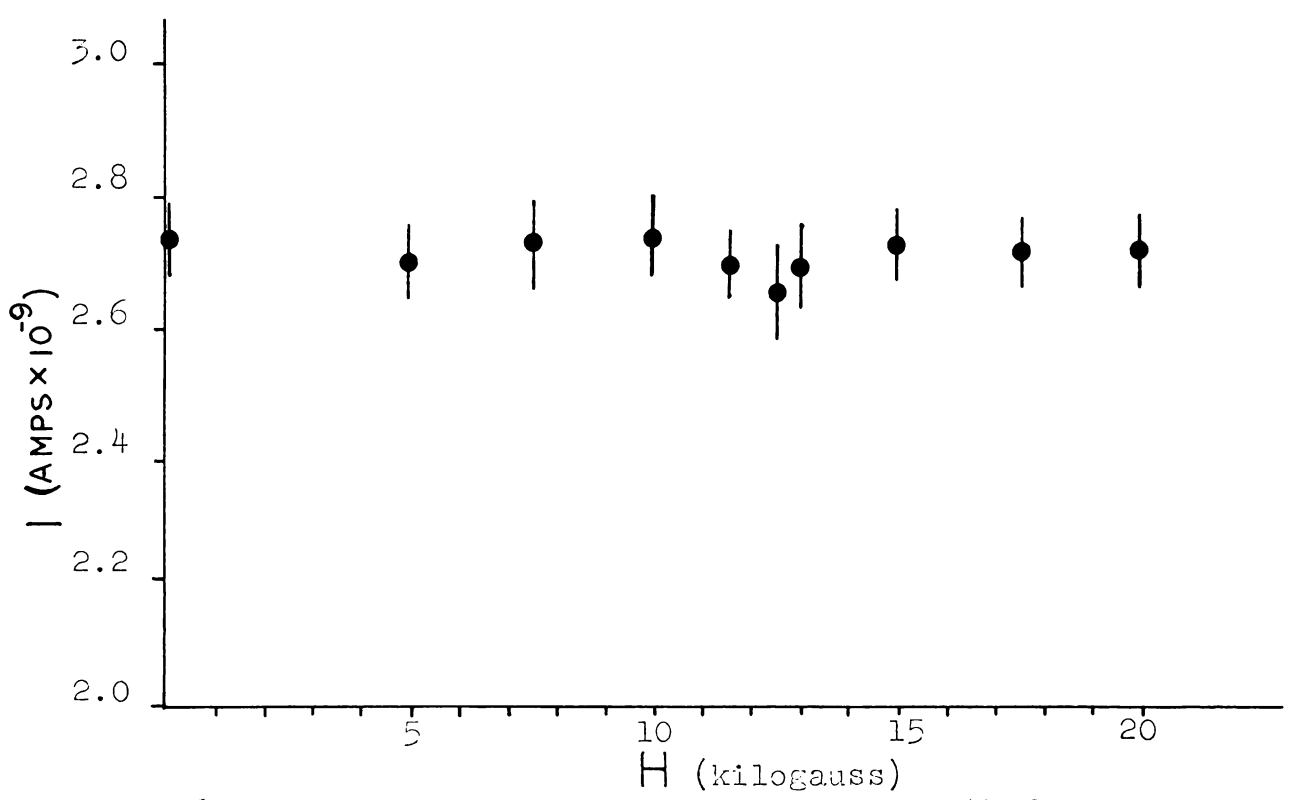


Figure 6 Field emission current from a zinc cathode.

Magnetic field oriented along (0001) direction.

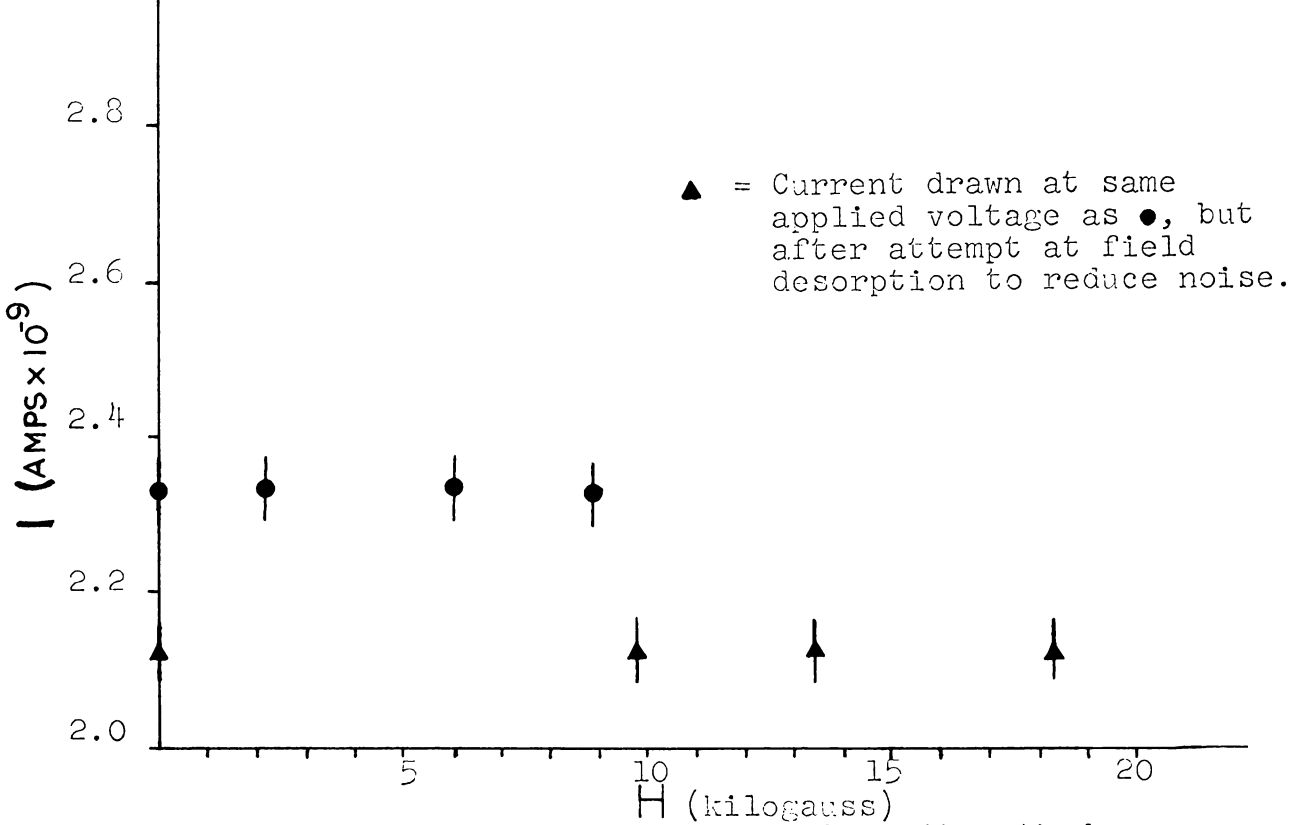


Figure 7 Field emission current from a bismuth cathode. Sample orientation unknown.



cannot be resolved without actually viewing the field emission pattern, and this, unfortunately, could not be done with the apparatus used.

As suggested in the theoretical section, suitably doped semiconductors should provide the necessary conditions for easily observing quantum effects in the field emission current. For this reason, some attempts were made using an emitter etched from n-type lead telluride. The particular sample used had an electron concentration of 10¹⁸ carriers per cm³. Since PbTe exhibits no band overlap, one would expect all the terms in eq. (116) to be made manifest, but again, to an accuracy of in this case approximately 2 per cent, no effect whatsoever was observed in the range O to 20 kilogauss. (The currents drawn from the PbTe cathodes were much more stable than those drawn from metallic cathodes, which accounts for the somewhat lower noise levels. fact the usual "training" period of several hours duration could almost be completely eliminated.) These results were typical of all of the attempts made to observe the phenomena, no matter what the cathode material happened to be. In the following section we shall present some possible causes for the apparent failure of the experiment.

Some of the current-voltage characteristics for a few of the various emitters used are shown in figures 8 through 11. A plot of this nature was always made at the start of each experimental run to ensure the fact that a field emission current was indeed being observed. (The

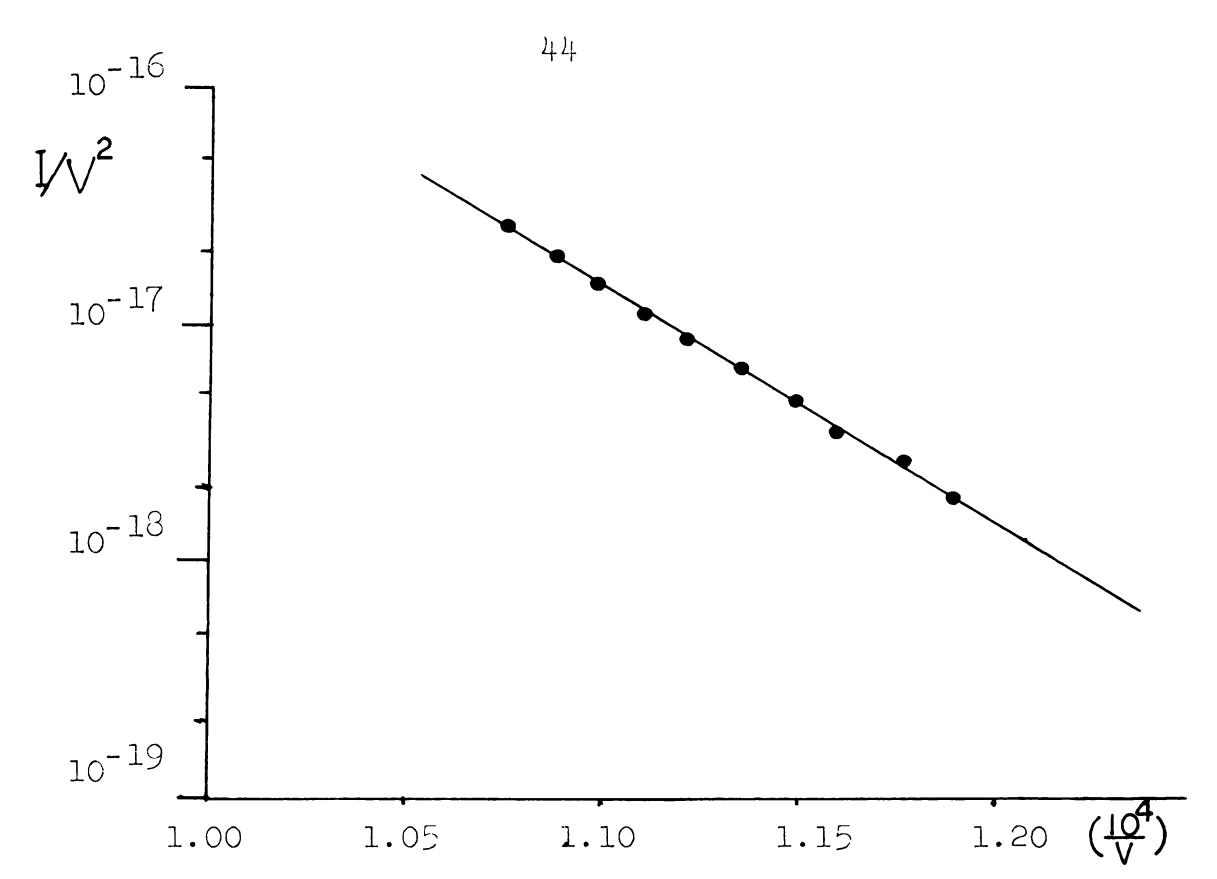


Figure 8 Current vs. voltage plot for a bismuth cathode in zero magnetic field. Sample orientation unknown.

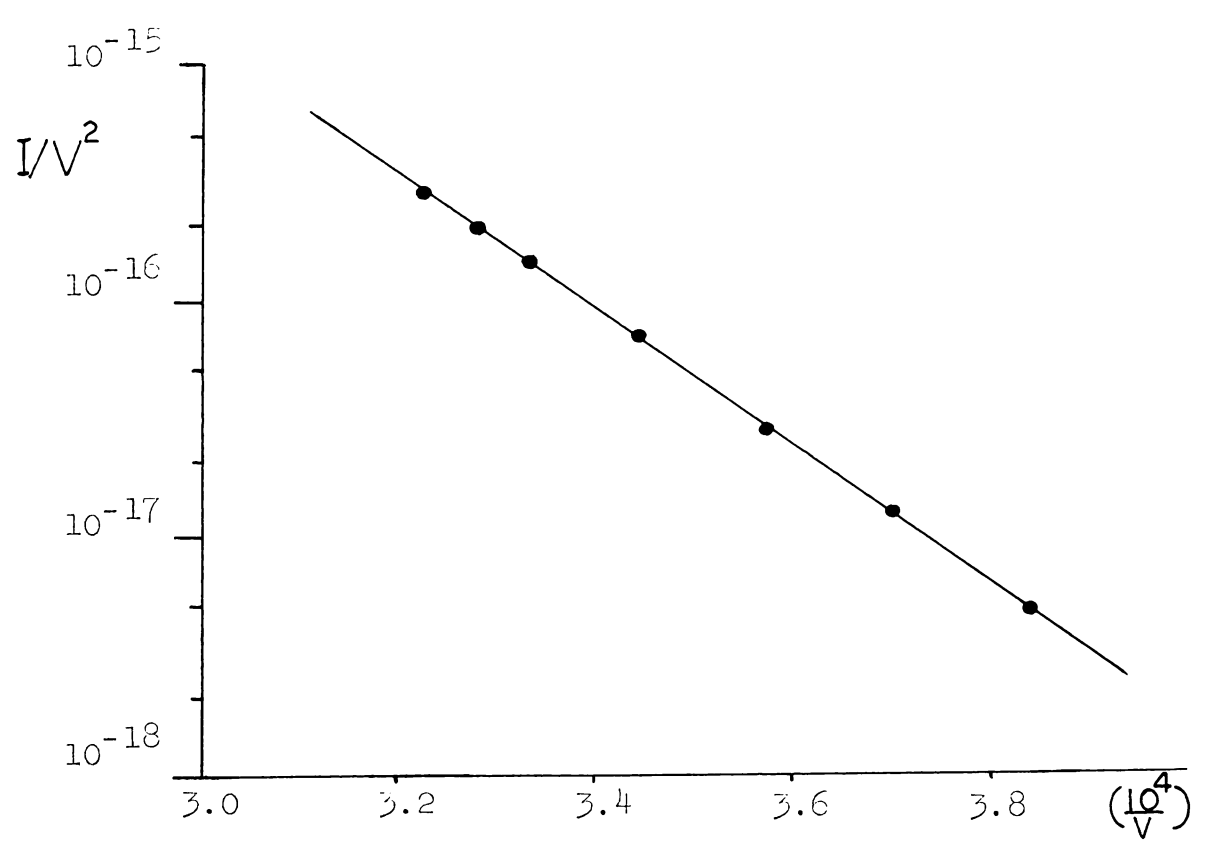


Figure 9 Current vs. voltage plot for a zinc cathode in zero magnetic field. Sample oriented along (0001).



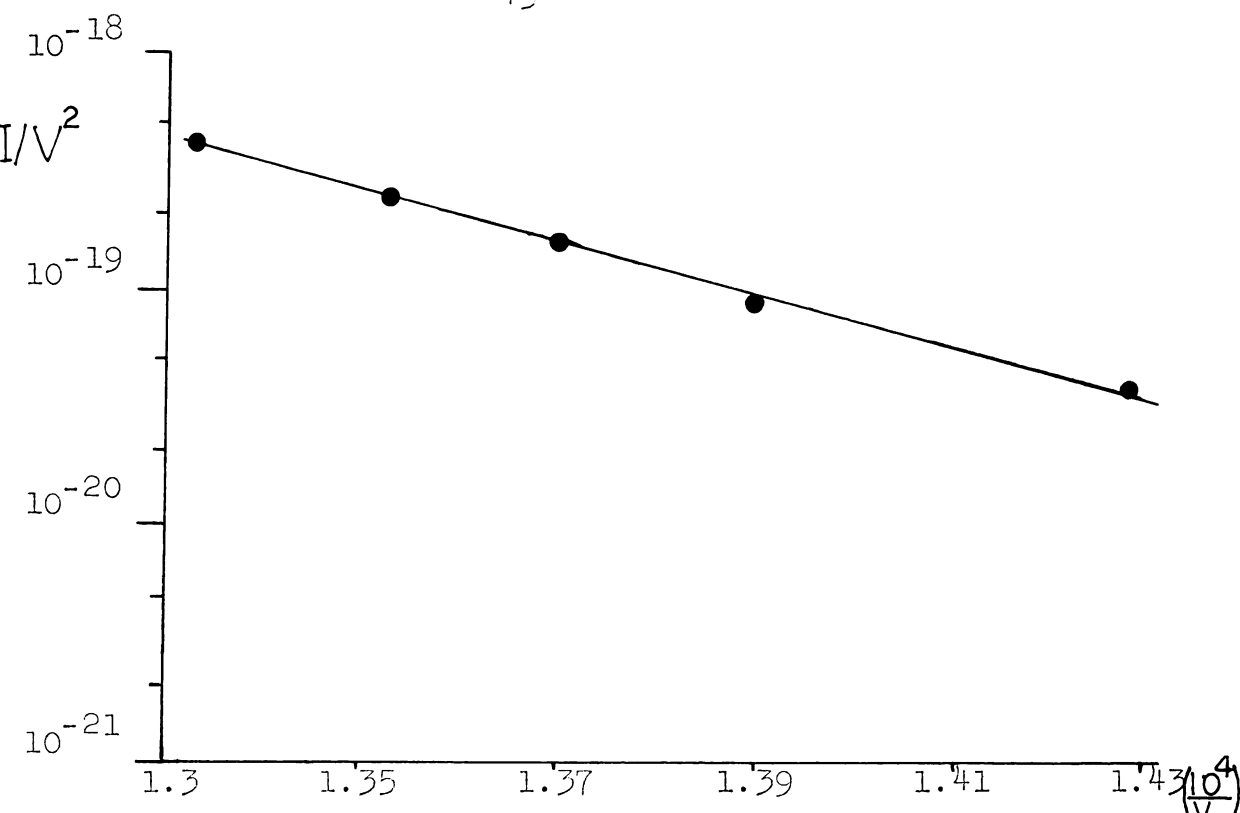


Figure 10 Current vs. voltage plot for a tungsten cathode in zero magnetic field. Sample orientation unknown.

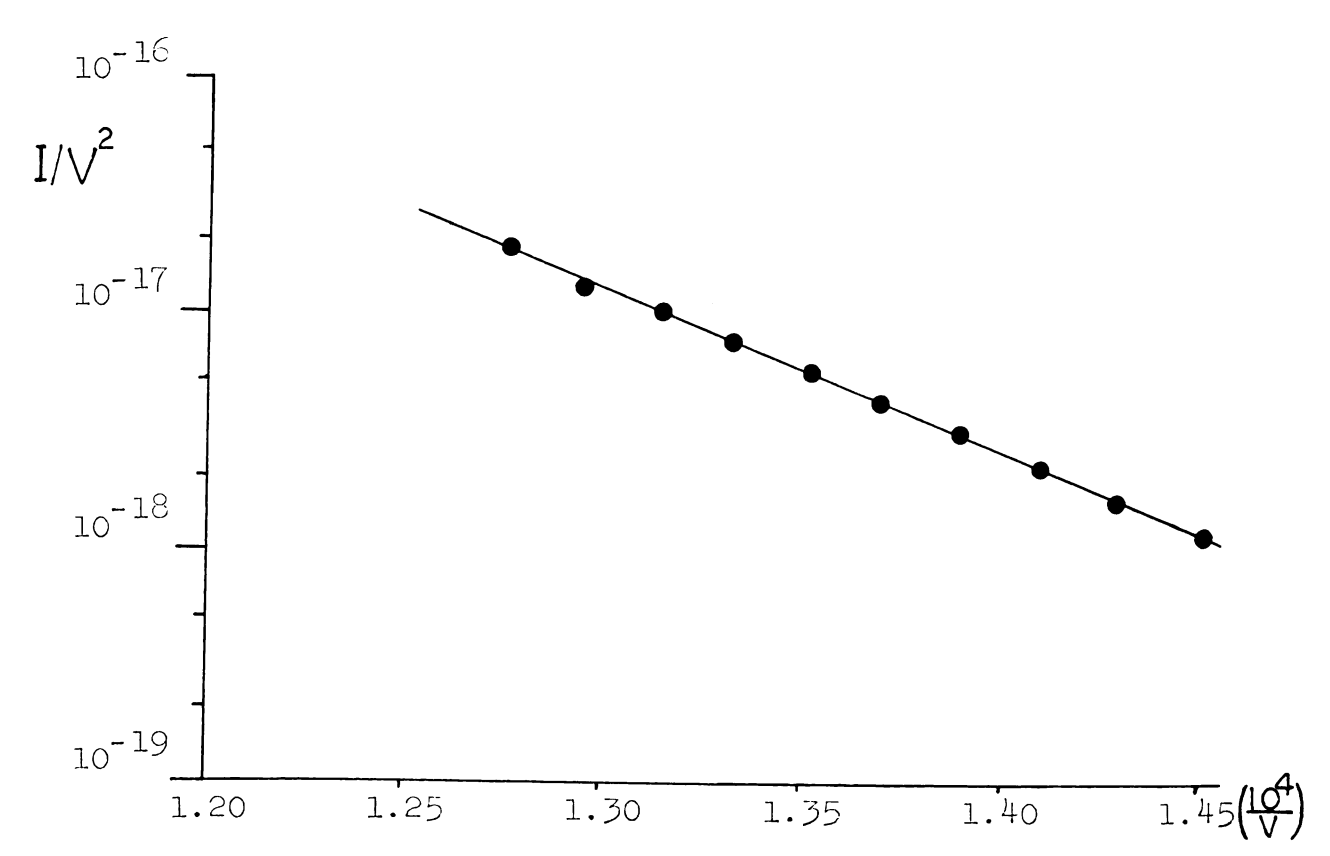


Figure 11 Current vs. voltage for a lead-telluride cathode in zero magnetic field. Emitter axis 28° from (111) direction.

F-N theory indicates that a plot of $\log (I/V^2)$ versus 1/V ought to be a straight line.) As mentioned above, this kind of plot was also used in some cases to intestigate the behavior of the current in a magnetic field. Whenever possible, however, the emission gap voltage was kept constant and the magnetic field was varied continuously in a linear fashion.

The F-N equation for the current density in zero magnetic field is

$$J = \frac{1.54 \times 10^{-6} F^2}{\text{ot}^2(y)} \exp -6.83 \times 10^7 \frac{0^{3/2}}{F} v(y)$$
 (118)

where y, v(y) and t(y) are defined in eqs. (29), (39), and (44) respectively. If the radius of curvature at the emitter apex can be determined, and a suitable approximation to the emitter geometry made, then the magnitudes of both J and F can be estimated. These values can be inserted in eq. (118) and used to determine the average work function of the cathode material as an additional check on the nature of the current observed. Unfortunately the necessary geometrical factors are very difficult to ascertain accurately after electrical breakdown across the gap occurs, and such an event almost inevitably took place sometime during each In only one run, other than that with Zn, were reliable data obtained before a breakdown occurred, and since an estimate of emitter geometry was always made prior to each run, we shall attempt to determine the magnitude of the work function for that emitter. The emitter was etched

from PbTe, and its I-V curve is shown in figure 11. The radius of curvature at the apex was estimated by means of an optical microscope to be 8×10^{-4} cm. Since the most significant contribution to the current comes from an area at the apex within about 45° of the emitter axis, 13) we can estimate that the current denisty corresponding to I = 7.7 $\times 10^{-10}$ amperes is J = 6.38 $\times 10^{-4}$ amps/cm². Assuming a hyperboloidal approximation for the cathode geometry 14) we find that

$$F = \frac{2V}{r \ln \frac{4s}{r}} = 4.95 \times 10^6 \text{ V/cm}, \tag{119}$$

where V=7700 volts is the anode potential, and $s\doteq.1$ mm is the cathode-anode separation. Substituting these values in eq. (118) and taking the logarithm of both sides yields

$$-25.3 + \text{Ln } 1.69 \phi = -13.8 \phi^{3/2} v(.843/\phi).$$
 (120)

A graphical solution of this equation gives ϕ = 1.8 eV, with an estimated accuracy of at best \pm 50 per cent. Most, if not all, of the uncertainty in the preceeding calculation comes from not being able to determine the geometry and dimensions accurately. Nonetheless, there is some merit in making this calculation, because it offers further evidence that an actual field emission current had been obtained. This fact is of some importance in the case of this particular emitter, because noise levels in the current were low enough to permit sweeping the magnetic field, at a rate of 1000 gauss/min, over nearly the full range of field

strengths available (0 - 20 kilogauss). As we mentioned previously, no dependence on magnetic field was found. (A similar calculation for the zinc cathode yeilds ϕ = 3.5 eV, again within the same limits of accuracy. The accepted value from photoelectric measurements is 4.24 eV. ¹⁵⁾)

•			

5. Conclusion

As an aid in determining possible reasons for the failure to observe a dependence of field emission current on magnetic field, we shall estimate numerically the magnitude of J when H equals 10 kilogauss. If the cathode material is bismuth, we note the following:

$$n = 1.57 \times 10^{-2} \text{ ev}$$
 (121a)

$$\phi = 4.25 \text{ ev}.$$
 (121b)

If we assume an electric field strength of $F = 2 \times 10^7$ volts/cm, then

$$d = 9.76 \times 10^{-2}$$
 (122a)

$$\eta/d = .161 \tag{122b}$$

$$e^{\eta/d} = 1.175$$
 (122c)

$$\hbar\omega/d = 1.1 \times 10^{-2}/9.76 \times 10^{-2} = .1127.$$
 (122d)

Since in this case the expansion parameters used in deriving eq. (116) are not particularly small, we must use eq. (106) instead. In order to simplify the calculation we shall consider only the first term in the series to estimate the size of the effect predicted. If anything, this will produce an over-estimate, for the second term, which is reduced by a factor of 4, will have the opposite sign. We have, then, neglecting also the term $(\hbar\omega/d) \sin\frac{2\pi\eta}{\hbar\omega}$,

$$J \doteq \frac{4\pi m^* ed}{h^2} \exp(-g - \frac{\eta}{d}) \left\{ (d(\exp(\frac{\eta}{d}) - 1) - \eta) - \frac{(\hbar\omega)^2}{2\pi^2 d} \left[\exp(\frac{\eta}{d}) - \cos\frac{2\pi r}{\hbar\omega} \right] \right\},$$
(123)

so that

$$\frac{J_{\text{osc}}}{J_{\text{steady}}} = \frac{3.27 \times 10^{-5}}{1.39 \times 10^{-3}} = 2.36 \times 10^{-2} . \tag{124}$$

From this we see that magnetic field effects are only on the order of 2 or 3 per cent of the emission current in zero magnetic field. This estimate, if at all correct, is itself enough to explain the apparent contradiction between experiment and theory - noise levels due to instabilities in the emission current were simply too large to allow the effect to be seen. It is immediately apparent that the experiment should be performed with magnetic fields in the range 50 to 100 kilogauss so that the field-dependent terms will be large enough to observe. Because of a mistake in a numerical estimate of the effect in the paper by Blatt, ll) it was originally felt that such high magnetic field strengths would not be necessary, particularly in bismuth. It now appears that this may not be the case.

In connection with the preceeding, we should mention that recent experiments 16) with Sb-doped germanium tunnel diodes have demonstrated an oscillatory dependence of the tunneling current on magnetic field. It is noteworthy to mention, moreover, that magnetic field strengths in the range 50 to 100 kilogauss were necessary to produce easily detectable oscillations, and in fact that at 10 kilogauss the effect was on the order of 2 per cent! Although the tunneling current in this case flows from a set of Landau levels on one side of the junction to a similar set on the

other side, the kind of calculation made is essentially the same as the one presented in the first part of this paper. One first considers the wave equation for the electron's motion in the junction region to obtain a transmission coefficient, and then computes an integral essentially of the form of eq. (72). (Harrison, 17) for example, has shown that in the WKB approximation, a general expression for the tunneling current density, based on an independent-particle point of view, is

$$j = \frac{2e}{h} \underset{k_t}{\searrow} \int_{-\infty}^{\infty} \exp(-2 \int_{x_a}^{x_b} \mathbf{k}_x \mathbf{k}_x) (f_a - f_b) dE , \qquad (125)$$

where f_a and f_b are the probabilities of occupation of the states a and b, k_t is the transverse wave number, $|k_x|$ is the magnitude of the electron's momentum perpendicular to the barrier, and $x_b - x_a$ is the extension of the forbidden region. The region to the left of the barrier is denoted by the subscript a, and that to the right by b. We can recognize eq. (72) in eq. (125) immediately if we set $f_b = 0$ for the probability of occupation of the vacuum states, and recall the form of $D(\varepsilon_z)$ given by eq. (22).)

There are, in addition to the foregoing, more reasons for the seeming contradiction between experiment and theory. For example, the expression we obtained for the energy levels of an electron in a magnetic field depended upon the assumption that the actual physical dimensions of the crystal were much greater than the classical orbit radius of an electron. This assumption neglects the effects of

those electrons whose orbit centers are close enough to the surface so that the electron paths intersect it. $\text{Dingle}^{10)} \text{ has shown that this is a valid procedure only }$ when

$$eHR/c > (2m*\eta_0)^{1/2}$$
 (126)

where R is the least dimension in a plane perpendicular to H. For a substance such as bismuth, eq. (126) requires that

$$HR > > 5 \times 10^{-2}$$
 (127)

According to the Fowler-Nordheim expression for the current density in the absence of an external magnetic field, an electric field of 2 X 10^7 volts/cm will produce a current density of approximately 5 X 10^{-3} amps/cm² assuming an average work function of 4.25 ev. In order to produce this field with a reasonable value of applied voltage, (say 5 X 10^3 volts), an emitter tip with a radius of curvature at its apex of about 5 X 10^{-5} cm is required. (We assume a hyperboloidal approximation to the cathode surface so that 14)

$$F = V \frac{2}{V \ln \frac{4s}{r}}, \qquad (128)$$

where V is anode potential, r is the radius of curvature, and s is the anode-cathode separation. With $s \doteq 1mm$, these conditions correspond to a current on the order of 5 X 10^{-11} amps.) We see immediately that we must have

$$H > 1000 \text{ gauss}$$
 (129)

in order to satisfy condition (127), and that for the most part it was not successfully met in this experiment. In fact, the orbit radius for electrons at the Fermi surface of bismuth is given by

$$r = (2m*_{\eta_0})^{1/2} \text{ c/eh} = 4.2 \text{ X } 10^{-2}/\text{H cm},$$
 (130)

For a field of 10 kilogauss, $r \doteq 4 \times 10^{-6}$ cm, which is almost one tenth of the estimated radius of the emitting region! Hence we must conclude that the applicability of our calculation is somewhat in question for the range of field strengths used. (Dingle¹⁸⁾, for example, has shown that for systems of small size the effect of these "surface states" (i.e. those containing electrons whose orbits intersect the surface) is to reduce the amplitude of de Haasvan Alphen oscillations.)

There is yet another question of a theoretical nature which deserves some attention. We mentioned above that changes in the Fermi level could be neglected if the number of electrons were allowed to vary, and that this could happen if a high density-of-states, heavy-mass hole band overlapped a light-mass conduction band. We then proceeded to investigate the nature of the current density, assuming that the only electrons which contributed to it originated from the conduction band. This procedure is probably justified when discussing the ordinary transport phenomena of bulk materials, such as the electrical and thermal conductivities, thermopowers, and so on, because the observed behavior of the electronic system will be

dominated by those electrons whose mobilities are highest. Whether or not an electron will contribute to a field-emission current, however, depends only on its energy relative to the top of the potential barrier, not on its mobility in the solid. On this basis it would appear that we are not justified in discussing only those electrons in the conduction band, but that the heavy-mass holes should be included as well. In fact it may well be that the predominant contribution to the current comes from the much higher density-of-states hole band, in which case any influence of the magnetic field on the emission current would be extremely difficult to detect. Recalling the form of the expression for the parameter d from eq. (46b), and using eq. (123) again for simplicity, we see that

$$J = \frac{4\pi m^* ed^2}{h^3} \exp(-g - \frac{\eta}{d}) \left\{ \exp(\frac{\eta}{d}) - 1 - \frac{\eta}{d} - \frac{1}{2} (\frac{\hbar \omega}{\pi d})^2 \left[\exp(\frac{\eta}{d}) - \cos \frac{2\pi \eta}{\hbar \omega} \right] \right\}$$

$$= \frac{e^3 F^2}{8\pi h \phi t^2(y)} \exp(-g - \frac{\eta}{d}) (\frac{m^*}{m_0}) \left\{ \exp(\frac{\eta}{d}) - (1 + \frac{\eta}{d}) - \frac{2\phi t^2(y) H^2}{\pi^2 c^2 F^2} \frac{m_0}{(m^*)^2} \left[\exp(\frac{\eta}{d}) - \cos \frac{2\pi \eta}{\hbar \omega} \right] \right\}.$$
(131)

This expression seems indeed to indicate that in zero magnetic field the emission current will primarily consist of electrons which, inside the metal, have the highest effective masses. In bismuth, for example, where $m^*/m_0 \doteq .57$ for the heavy-mass nearly-filled band, ¹⁹⁾ and $m^*/m_0 \doteq 10^{-2}$ for the light-mass conduction band, it would appear that

the high-mobility electron band contributes only about 1.6 per cent of the total current. This presents a most unfortunate situation, for when a magnetic field is applied we see that

$$\frac{J_{\text{osc}}}{J_{\text{steady}}} = \frac{2\phi t^{2}(3.79 \text{ X } 10^{-4} \frac{\text{F}^{1/2}}{\phi}) \text{H}^{2}}{\pi^{2} c^{2} \text{F}^{2} \left[\exp\left(\frac{\eta}{d}\right) - \left(1 + \frac{\eta}{d}\right) \right]} \frac{m_{o}}{(m^{*})^{2}}$$

$$= 2.39 \text{ X } 10^{-41} \text{ H}^{2} \frac{m_{o}}{(m^{*})^{2}}, \qquad (132)$$

assuming an electric field strength of 2×10^7 volts/cm. Hence, in a magnetic field of 20×10^7 kilogauss,

$$\frac{J_{osc}}{J_{steady}} = 3.2 \times 10^{-5}$$
 (133)

for the heavy-mass electrons. If this is actually the case, then it is not surprising that we failed to observe any influence of the magnetic field on field emission in this experiment.

This, however, is not the end of our discussion, because the experiment was also tried using n-type PbTe for the cathode, with the same results. Since there is no band overlap in this substance, and since $m^*/m_0 \doteq .05$, the objections of the preceding paragraph do not apply. The first suggestion that the size of the effect was just too small at the field strengths used is of course still valid, but there is yet another problem which merits consideration. The possibility exists that all of the cathodes contained adsorbed gases on their surfaces. It is well known that

adsorbed gases change the effective work function at the surface of the emitter, essentially by the formation of a dipole layer. The direction of the change in work function depends upon whether or not the adsorbed substance is electronegative or electropositive. The former causes an increase in the effective work function and hence a decrease in the emission current, and vice versa for the latter. In either case, the following picture has emerged from field-emission studies of adsorption on cathode surfaces. 20) It is assumed that a molecule next to the surface of a metal may be represented by a potential well containing some bound states, a forbidden zone, and an unoccupied band above it. If the ionization potentials are higher than the work function of the substrate metal, the occupied zone of the molecule will lie below the Fermi level of the metal (figure 12a). The application of a strong electric field will cause the energy levels of the molecule to be tilted so that there are now unoccupied states below the Fermi energy. These states can be filled very easily by substrate electrons tunneling through the forbidden zone. In such a case the electrons in these newly-filled states then tunnel through the rest of the barrier to provide a field emission current (figure 12b). The only requirement is that the substrate metal be able to supply with ease the electrons needed to fill the molecular states. significant aspect of such a picture is that now electrons in the metal which are not necessarily near the Fermi

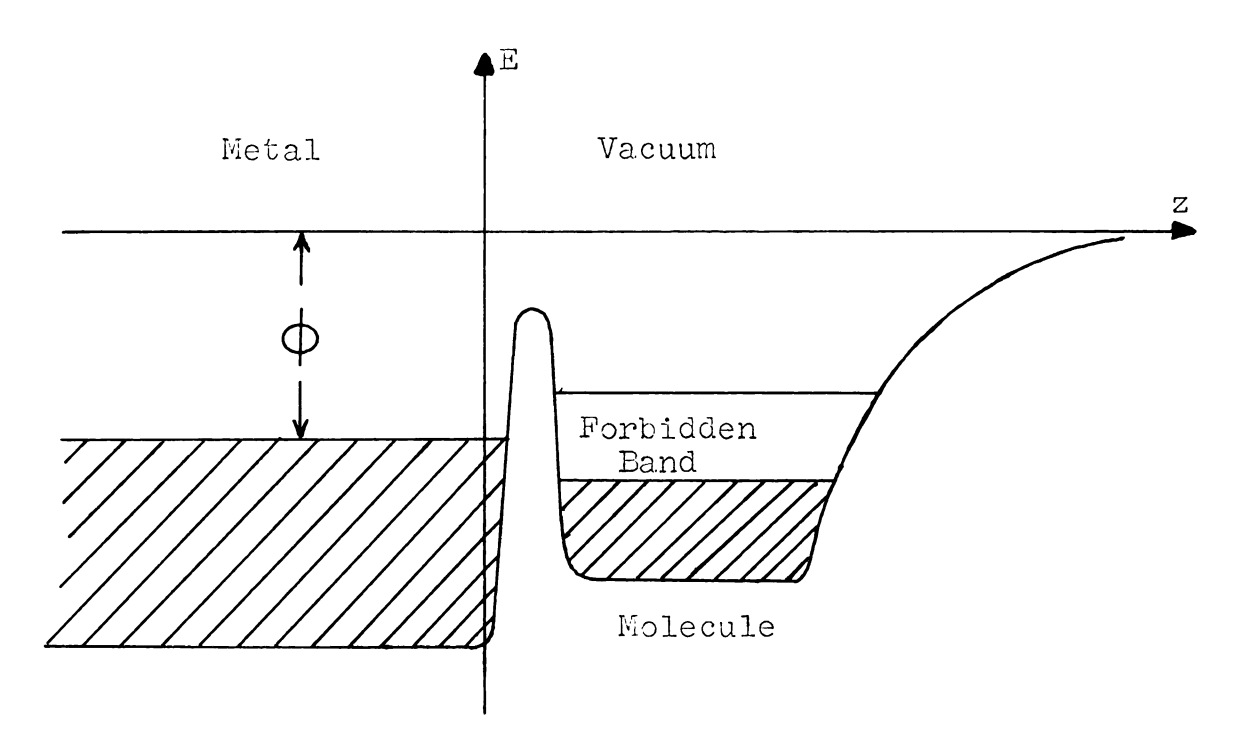


Figure 12a Molecule near a metallic surface in zero applied electric field.

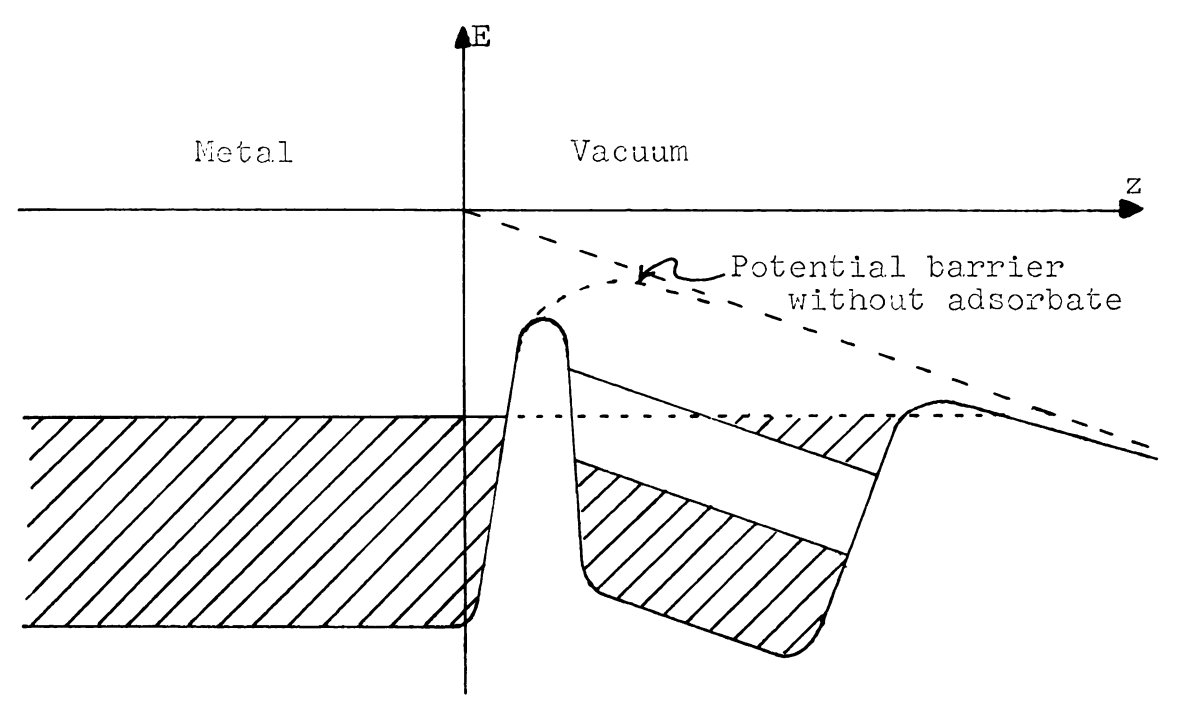


Figure 12b Molecule near a metallic surface with an applied electric field.

surface may contribute significantly to the emitted current, since the potential barrier has effectively been reduced by a considerable amount. Unless the magnetic field can somehow drastically alter the population of the energy levels inside the metal, we would not expect to observe any quantum oscillations in a field emission current of this sort.

Perhaps we should pause here for a moment and state a fact which may have been overlooked in all of the above. That is, electrons which make the main contribution to a field emission current must necessarily come from the lowest Landau levels in the metal. This follows from the requirement that the energy of an electron for motion perpendicular to the barrier must be as large as possible so that the penetration probability will be a maximum. Noting this in connection with the above, it is easy to see how the emitted current will not be affected to any great extent by a magnetic field, for not until the extreme quantum limit is reached will the population of the lowest Landau levels be significantly altered. In fact it is this situation which makes the estimated magnitude of the effect so small, contaminated surfaces notwithstanding. The populations of the lowest Landau levels will not undergo the large and sudden (at 0 oK) changes which occur in those of the levels near the Fermi surface when they are finally forced above it by the magnetic field. This is completely different from de Haas - van Alphen



or magnetothermal oscillations. In these two cases only electrons in the Landau levels nearest the Fermi level can contribute, so when the magnetic field causes one such level to depopulate, a much stronger effect should, in principle, be noted.

We shall close this series of speculations by making one more. It seems to be apparent that the best chance one has of observing quantum oscillations in a field emission current is to use a substance which has no overlapping bands, small effective masses, and which does not readily undergo chemical reactions. Such a substance may possibly be found among suitably doped n-type semiconductors, such as, for example the PbTe used in this experiment. (The preceeding suggestions may well be the reasons why, for example, oscillations were observed in the tunneling current in the germanium tunnel diode mentioned above. Properly doped germanium fulfills the requirements guite well.) The last requirement is that the experiment be performed in magnetic fields in the range 50 to 100 kilogauss. Practically all of the above objections (eg. eq. (126) and ensuing discussion) can then be avoided. It is hoped that someday this will be done.



References

- 1) R.W. Wood, Phys. Rev. <u>5</u> 1 (1897)
- 2) W. Schottky, Z. Physik <u>14</u> 63 (1923)
- 3) R.A. Millikan and C.F. Eyring, Phys. Rev. 27 51 (1926)
- 4) Millikan and Lauritsen, Phys. Rev. 33 598 (1929)
- 5) R.H. Fowler and L. Nordheim, Proc. Roy. Soc. (London)
 All9 173 (1928)
- 6) L. Nordheim, Proc. Roy. Soc. (London) <u>A121</u> 626 (1928)
- 7) E. Merzbacher, Quantum Mechanics, Wiley and Sons, 1961, pp 118
- 8) R.E. Burgess, H. Kroemer, and J.M. Houston, Phys. Rev. 90 515 (1953)
- 9) R.H. Good Sr. and E.W. Mueller, in <u>Handbuch der Physik</u>, Edited by S. Flugge, Springer-Verlag, Berlin (1960) pp 186
- 10) R.B. Dingle, Proc. Roy. Soc. (London) <u>A211</u> 500 (1952)
- 11) F.J. Blatt, Phys. Rev. <u>131</u> 166 (1963)
- 12) J.J. Lepage, Thesis, Michigan State University (1965)
- 13) Dyke, Trolan, Dolan and Grundhauser, JAP 25 106 (1954)
- 14) R.H. Good and E.W. Mueller, Ibid., pp 192
- 15) C. Kittel, <u>Introduction to Solid State Physics</u>, 2nd ed., Wiley and Sons, (1954)
- 16) Roth, Bernard and Straub, Phys. Rev. <u>145</u> 667 (1966)
- 17) W.A. Harrison, Phys. Rev. <u>123</u> 85 (1961)
- 18) R.B. Dingle, Proc. Roy. Soc. (London) <u>A219</u> 463 (1953)
- 19) Grenier, Reynollus, and Sybert, Phys. Rev. <u>132</u> 58 (1963)
- 20) W.P. Dyke and W.W. Dolan, Adv. in Electronics, 8 New York, Academic Press (1956)



